Modelling of multiphase flow through a subsea recirculation line equipped with a choke

Joseph Onyeabor Ogechukwu

Master of Science

Thesis in Energy & Process Technology

Department of Physics and Technology

University of Bergen

February 2023

Abstract

A peculiar problem encountered in engineering practices for multiphase flows is the pressure loss in piping systems. Because of the variations in viscosities, densities, and velocities of the fluid phases, multiphase systems design requirements are different from those of single-phase flows. Irrespective of the number of phases involved, pressure loss occurs at different points of the pipe. The severity is however more in multiphase flows due to the variations in the fluid compositions across the length of the pipe. Works of literature on the pressure drop across chokes or valves for multiphase fluids are very limited due to the complexities and flow regimes bothered around the valve system. Moreso, most researchers only bother with the frictional losses along the pipeline as these are considered to constitute most of the losses. Current practices are only just interested in designing and sizing valves based solely on the pressure drop across a valve for single-phase flows. In this work, Daniel Bernoulli's model or equation was evaluated against empirical data from OneSubsea company in a bid to predict the pressure drop across a choke in a subsea recirculation line for multiphase flow. The equation was used to quantify and evaluate the performance characteristics of a valve handling multiphase gas-water-oil flow, as this kind of flow is commonly seen in processing industries. The received measured data include a 6-in-diameter pipe, with 60 meters equivalent length, and twenty-six bends. Stem travel from 7.1% to 70.5% for a recirculation pipe was evaluated against 118 data values of Gas Volume Factor GVF and Water Liquid Ratio WLR to obtain the control valve coefficients at different flow rates under varying temperatures and pressure. The results showed a good correlation in line with the principle of energy conservation or continuity equation when the flow rate 'Q' was measured against the pressure drop across the valve. Other quantitative relationships evaluating the effects of GVF, Bulk density of the fluids mixture against the pressure drop across the valve were also determined. The detailed evaluation carried out allows for local flow characteristics of pressure drop, flow rates, and GVF determination within the valve. The parameters can be incorporated in the sizing methodology of control valve systems for multiphase oil-water-gas flow.

Keywords: Multiphase-flow, Pressure drop, Re-circulation pipe, Choke

Acknowledgment

This project report is a prerequisite for a master's degree in Energy and Process Technology at the department of Physics and Technology, University of Bergen (UiB). The project was done in collaboration with OneSubsea Company.

I would like to thank first my Supervisor at the University of Bergen, Professor Pawel Jan Kosinski for his excellent support, and show of interest during the thesis period and Merry Ho for being an exceptional advisor. I would also like to profoundly thank my supervisor at OneSubsea, Emah Ebechue for his invaluable support, suggestions, and access to data from OneSubsea, used in the project realization. And of course, my sincere gratitude to the Digital Operations Department Manager at OneSubsea for allowing this collaboration, the experience garnered over the time of working on this thesis cannot be quantified.

Finally, I am especially grateful to my parents, my family, and my friends for their continuous support and endless encouragement.

23rd February 2023

Signature:

Joseph Onyeabor Ogechukwu

Nomenclature

Cv	Control Flow coefficient
Pin	Pressure inlet (bar)
dP	Differential Pressure (bar)
Q	Flow rate ($\frac{m^3}{hr}$)
S. G	Specific Gravity
WLR	Water Liquid Ratio
GVF	Gas Volume Factor
ρ_{mix}	Density mix ($\frac{kg}{m^3}$)
Kv	Flow coefficient
F	dimensionless friction factor
g	gravity constant ($\frac{m}{S^2}$)
V	Velocity ($\frac{m}{S}$)

Contents

INTRODUCTION 1

1.1 BACKGROUND OF STUDY 1

1.2 Objectives of the study 1

1.3 Organisation of this thesis 2

Chapter 2 5

2.1 GENERAL THEORY 5

2.2 Single-Phase flow 6

2.2.1 Energy of a Flowing Liquid and Bernoulli's Equation 6

2.2.2 Pressure Loss in Pipes 7

2.2.3 Darcy Friction Factor 7

2.2.4 Laminar flow 8

2.2.5 Transitional flow 8

2.2.6 Turbulent flow 8

2.2.7 Moody chart 10

2.2.8 VISCOSITY 11

2.3 Multiphase flow: 12

2.3.1 Flow patterns: 12

2.3.2 Plug flow: 13

2.3.3 Churn flow: 13

2.3.4 Annular flow: 13

2.4 Control Valves 15

2.4.1 Flashing and Cavitation 17

2.4.2 Choked Flow 19

2.4.3 Non-Choked flow: 19

2.5 Literature reviews 19

Chapter 3 22

3.1 METHODOLOGY 22

3.2 Models of Data Analysis 22

3.2.1 Method 1: 22

3.2.2 Method 2: 23

Chapter 4 25

4.1 RESULTS 25

Chapter 5 30

5.1 DISCUSSION 30

Chapter 6 ... 31
6.1 CONCLUSION AND RECOMMENDATION ... 31
REFERENCES ... 32
APPENDICES ... 34

LIST OF FIGURES

Figure 1: A description of pressure loss in pipes(Tec-Science, 2020) 4
Figure 2: a) Laminar flow .... b)Turbulentflow9
Figure 3: Moody chart diagram for friction factor determination 10
Figure 4: A stress-strain relationship for viscosity 11
Figure 5**: Flow regime diagram**..14
Figure 6: Horizontal flow regime diagram 15
Figure 7: A representation of a choke system (https://neutrium.net/fluid-flow/pressure-loss-cv-and-kv-method/)..16
Figure 8: An illustration of flowing pressure drops through a choke. 18
Figure 9: A graphical representation of Flow rate against the pressure drop. ....**Error! Bookmark not defined.**
Figure 10: A representation of Q VS Pressure drop for avg. inlet and outlet density mixture. 26
Figure 11: A representation of gas bulk density against dP 27
Figure 12: An illustration of fluid viscosity vs dP..28
Figure 13: Graph of liquid bulk density against obtained pressure drop.................................29

INTRODUCTION

1.1 BACKGROUND OF STUDY

Multiphase flow, the simultaneous flow of two or more immiscible phases, is a common occurrence in various industrial processes such as oil and gas production and transport, power generation, and chemical processing. In these systems, the pressure loss of multiphase flow through a recirculation pipe is a crucial factor to consider when designing and operating the system. The pressure loss in a recirculation pipe can be caused by several factors, including the viscosity and density of the fluids, the flow rate, and the pipe geometry.

"When fluids flow through pipes, energy losses inevitably occur"(Tec-Science, 2020). The Energy (pressure) losses are resultant efforts geared at overcoming all resistances encountered as the fluids flow through the pipe. In the practical analysis of piping systems, the quantity that is considered most vital is the pressure loss. Pressure losses occur due to form and wall frictional effects along the length of a piping system, as well as at other components of the piping system like fittings, valves or chokes, piping entrances, bends, etc. Since the basis for fluid flow in pipes is the pressure gradient, a permanently decreasing pressure is therefore formed along the pipe in the direction of flow.

In general, the accuracy in predicting pressure losses involved with this kind of flow seems to be a herculean task. Therefore, a good understanding of frictional characteristics as well as losses at other components (which are the basis for pressure loss) in pipes is essential since it could improve the accuracy of design and optimization of the process systems (Xu et al., 2014).

When the fluid is a multiphase mixture as we intend to consider, such as oil-gas-water, the pressure loss can be more complex and difficult to predict. "This is due to the significantly different densities and viscosities of the phases. The flow behaviors are also predictably more complicated by the complex heat transfer that occur as the fluids flow through the piping system when pressure and temperature changes"(Brill, 2010). The complexities associated with the multiphase flow are what make them more interesting.

1.2 Objectives of the study

Only in recent years have researchers begun to consider the basic flow hydrodynamic phenomena involved in multiphase flow and to develop theoretical models for determining the flow characteristics and constraints like pressure gradient (Ansari & Sylvester, 1988). Although previous studies have sought to understand the complexities involved in multiphase flow, a comprehensive analytical mechanism underlying the behavior of these fluids, to a varying degree remain un-investigated or collected in a convenient place.

As described above, the complexity of the pressure gradient over the length of the pipe differs considerably for a multiphase flow. The pressure and velocity distributions at different spatial locations of the piping system are critical for effective heat transfer, mixing, and circulation. Further, studies have shown that multiphase flows allow more pressure losses than single-phase flows. What Engineers seek therefore is to establish a sound economic principle that helps reduce cost while maximizing profit and productivity. From an economic standpoint, accurately predicting these losses may reduce the pumping energy needed for the fluid delivery to the destination in long pipelines.

Flow measuring meters are normally positioned for calculating pressure losses across the length of a pipe. However, there are no measuring meters for calculating accurately pressure losses across the chokes in a pipeline. And because of the complexities surrounding multiphase flows, there is just limited research done in this area. It is important to know that minor losses in long pipes may be ignored but not when they arise from part open valves, they are often significant and should not be ignored. Our main objective therefore is to evaluate a suitable model that can give good prediction of those losses across the choke in a recirculation line.

With the analytical approach, our objective also will be to have a good understanding of the multiphase flow dynamics with the aim to investigate the pressure loss through a recirculation pipe. Understanding and predicting fluid pressure profile in pipes especially across the choke is important for the design and operation of pipelines and oil and gas production systems.

1.3 Organisation of this thesis

The structure of the remainder of the thesis is outlined as follows:

Chapter 1 involves an overview of this thesis. It includes a general introduction to the pressure drop in piping systems especially for a multiphase flow system. Furthermore, it contains the problem statement, objectives, and scope.

Chapter 2 gives a detailed theoretical analytical review of the pressure drop in single and multiphase flows. Detailed work on flow patterns associated with pipes with inclination and across chokes. Deals extensively with review of flow patterns, flow maps and void fraction correlations of multiphase flows.

Chapter 3 contains the methodology of this project. It shows a stepwise approach to deriving the formula to calculate pressure drop across the entire length of the pipe but with great focus on the choke system.

Chapter 4 will seek to present and analyse results obtained based on the model formulated for pressure loss prediction across a choke for multiphase flow in a recirculation line. It elaborates the performance analysis of the model in correlation with industry standard by incorporating data obtained from the industry.

Chapter 5 is the concluding part of the thesis. It draws attention to what is being achieved, the possibilities of the model evaluated , and future recommendations for research.

Figure 1: A description of pressure loss in pipes(Tec-Science, 2020)

Chapter 2

2.1 GENERAL THEORY

In this section of the thesis, we need to comprehend what and how pressure losses occur as well as to make sense of all the mathematical models and parameters that were used.

As earlier discussed, the viscosity and density of the fluids contribute largely to the pressure loss as they affect the fluid's resistance to flow, while the flow rate and pipe geometry determine the fluid's velocity and the amount of turbulence in the pipe respectively. This effect is more pronounced in multiphase fluids as the viscosity of the separate phases can vary greatly. Pressure losses resulting from frictional effects are categorized as major losses while those resulting from other pipe components such as the fittings are termed minor losses.

Moreso, modelling the pressure loss of multiphase flow through a recirculation pipe can be challenging due to the complex interactions between the different fluid phases. We therefore intend to do a brief review on recent studies of the subject matter, defining the important parameters employed while also elucidating the approach and the models used in calculating pressure losses in pipes for single and multiphase flows.

There are different approaches to predicting pressure losses in pipes whether single or multiphase flows such as the empirical, analytical, and numerical simulation methods. A common method which is the empirical approach, uses experimental data to determine the pressure loss. However, this approach can be time-consuming and expensive, especially for complex systems.

Another method is the analytical approach, which uses mathematical equations such as Darcy-Weisbach equation to relate the pressure loss to the fluid velocity, the pipe diameter, and the friction factor (a function of the flow regime). Another method is the use of the Moody chart, which relates the friction factor to the Reynolds number and the relative roughness of the pipe. And by extension, the two-phase flow pressure drop prediction method can be applied to estimate the loss in a recirculation pipe. The analytical approach can provide a more accurate prediction of the pressure loss but requires a detailed understanding of the fluid dynamics and the system geometry.

A more sophisticated approach would be to use Computational Fluid Dynamics (CFD) Simulations to solve **Navier-Stokes equation**, thereby simulating the flow behaviours, and predicting the pressure loss, but it requires large computational time and high-performance computer whose results are also subject to measurable errors.

Interestingly, any of these methods can be combined to measurably predict the pressure loss. An example would be a careful study that would allow us to evaluate empirical data from oneSubsea with Bernoulli equation for the distribution as this thesis intends.

In piping, it is necessary for engineers to know how much control they have over the fluids flowing in pipelines. (Griffith, 1984) explains that depending on the application of the pipe, (the following questions which are of importance to this study) would arise:

- What is the void fraction of the phases involved?
- What is the pressure loss in the pipeline during the flow?

In our quest to understanding and the problems associated with flow in pipes, we will begin with a detailed study of flow types.

2.2 Single-Phase flow

This is a single kind of flow in pipes. Such could be oil, water, or gas. The concept of fluid flow in pipes works on the principle of conservation of energy and Bernoulli's equation. The energy equation assists in calculating so many characteristics associated with fluid flow, and in this case, Head loss or Pressure loss. The primary challenge confronting fluid engineers is deciphering pressure loss with greater accuracy. It has been established that pressure losses result from two major sources which we would look at in detail.

- frictional effects between fluid and pipe wall, and viscous forces within the fluid.
- Pipe geometry such as the fittings, elbows, valves etc.

2.2.1 Energy of a Flowing Liquid and Bernoulli's Equation

A steadily flowing fluid through a pipe is characterised by three components of energy:

- Potential energy due to liquid pressure
- Kinetic energy due to velocity
- Gravitational potential energy due to elevation

Conservation of energy is a principle that relates energy to only being converted from one form to another. Bernoulli's equation which is a form of this same principle states that if no energy is added or removed from the system along a streamline, the sum of the 3 energy components remains constant.

$$P + \rho\frac{\overline{V}^2}{2} + \rho g Z = CONSTANT \quad (2.1)$$

The assumptions for this equation lie on the system being incompressible, frictionless, steady, and no heat added or lost in the process. In practice however, no system exists with such assumptions, hence, an inclusion of head loss, pump head and a correction factor for uniform velocity distribution in a modified Bernoulli's equation for real applications.

$$\frac{P_1}{\rho} + \alpha_1 \frac{\overline{V}_1^2}{2} + gZ_1 + h_p = \frac{P_2}{\rho} + \alpha_2 \frac{\overline{V}_2^2}{2} + gZ_2 + h_f \qquad (2.2)$$

$$where\ P\ is\ the\ pressure\ head, \rho \frac{\overline{V^2}}{2}\ is\ the\ velocity\ head\ and\ \rho g Z\ is\ the\ elevation\ head.$$

$$h_f\ representing\ head\ loss, h_p\ as\ heap\ pump\ while\ \alpha_1\ \&\ \alpha_2\ are\ correction\ factors\ for\ vel.dis.$$

2.2.2 Pressure Loss in Pipes

(Khaleefa Ali, 2019) Pressure loss in a pipe, which is associated with frictional energy loss per length of the pipe, depends on the flow velocity, pipe length, pipe diameter, and a friction factor based on the roughness of the pipe and the flow regime (i.e., using the Reynolds number). "To calculate the pressure loss in a pipe it is necessary to compute a pressure drop, usually in fluid head, for each of the items that cause a change in pressure." But first, a simplified Bernoulli equation will yield:

$$\Delta P = \rho h_f \qquad (2.3)$$

Darcy Weisbach equation defines frictional head loss as:

$$h_f = f_D \cdot \frac{L}{D} \cdot \frac{\overline{V}^2}{2g} \text{ (Major losses)} \qquad (2.4)$$

$$h_f = \sum K . \frac{\overline{V}^2}{2g} \text{ (Minor losses)} \qquad (2.5)$$

Where K is known as the resistance coefficient for calculating the losses due to the pipe geometry (elbows, chokes etc.). It is important to know that fittings such as elbows, tees and valves contribute a significant pressure loss in most pipe systems and therefore should not be neglected.

2.2.3 Darcy Friction Factor

The Darcy friction factor is a dimensionless number used to determine the frictional head loss in a pipe. It is determined by using either the appropriate friction factor relative to the fluid's flow regime (Laminar or Turbulent flow regimes), or by reading off from a Moody Chart. The flow regime is determined by Reynolds Number.

2.2.4 Laminar flow

A laminar flow is one characterized by low or uniform velocity in the flow direction and whose Reynold's number is low (less than 2100). The Darcy equation for determining the Reynold's number is:

$$\mathrm{Re} = \frac{\rho \bar{V} D}{\mu} \quad (2.6)$$

$$\mathrm{Re} < \sim 2100 \quad (2.7)$$

$$f_D = \frac{64}{Re} \quad (2.8)$$

2.2.5 Transitional flow

This is a flow regime with inconsistency of flow pattern, hence, difficult to predict the friction factor.

There is no sufficient model to describe the flow regime just yet

2.2.6 Turbulent flow

A turbulent flow is characterized by high Reynold's number. Colebrook White equation remains by far the most accepted method for calculating the friction factor for this flow regime. This being that it puts into account results for the flow through smooth or rough pipe. Other equations by Serghide's, Chen's, Haaland, Zigrang etc. are all mere approximations of the Colebrook equation with some error in accuracy. Below is the Colebrook's equation for obtaining friction factor value which might require series of iterations.

$$Re < \sim 2300 \text{ and } Re > \sim 4000 \quad (2.9)$$

$$\frac{1}{\sqrt{f}} = -2log_{10}\left(\frac{\varepsilon/D_h}{3.7} + \frac{2.51}{Re\sqrt{f}}\right) \quad (2.10)$$

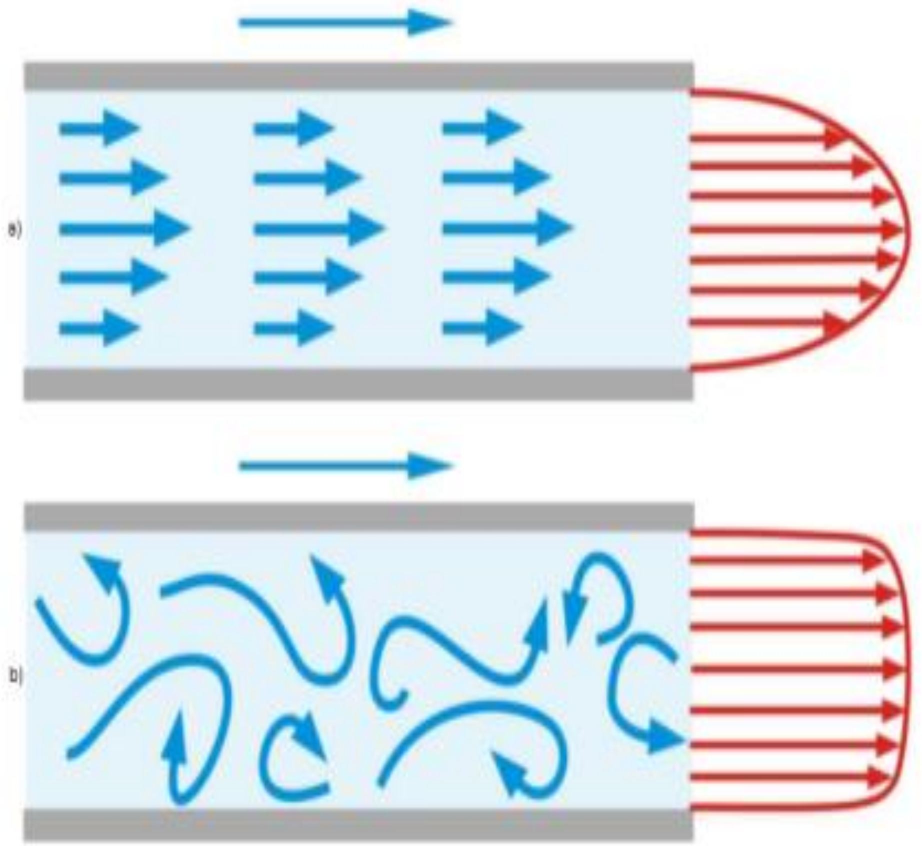

Figure 2: a) Laminar flow   b) Turbulent flow

2.2.7 Moody chart

As earlier pointed out, another common method for determining the friction fraction is by reading off the values from the Moody diagram or chart as seen below.

Figure 3:

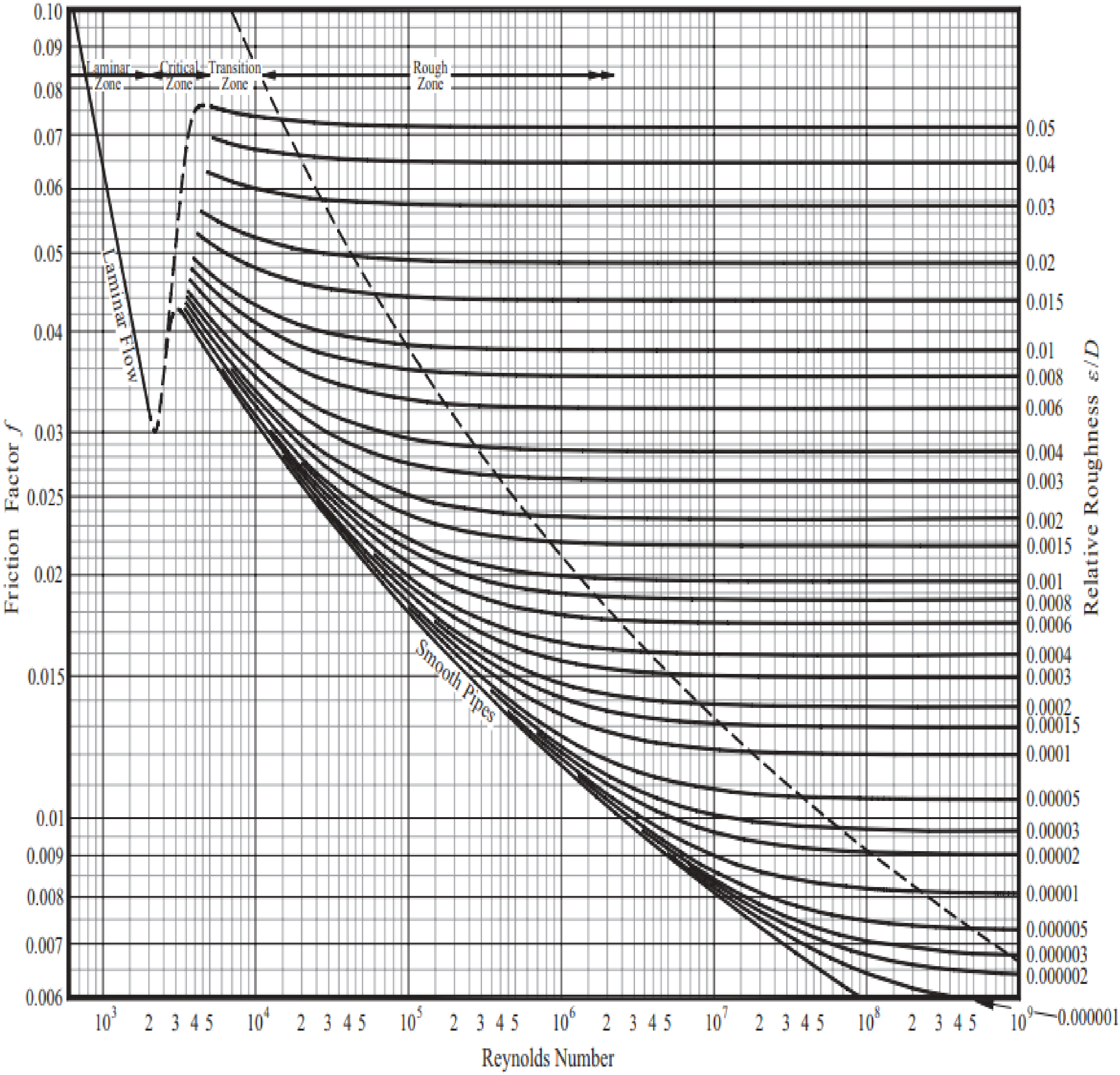

Figure 3: Moody chart diagram for friction factor determination

2.2.8 VISCOSITY

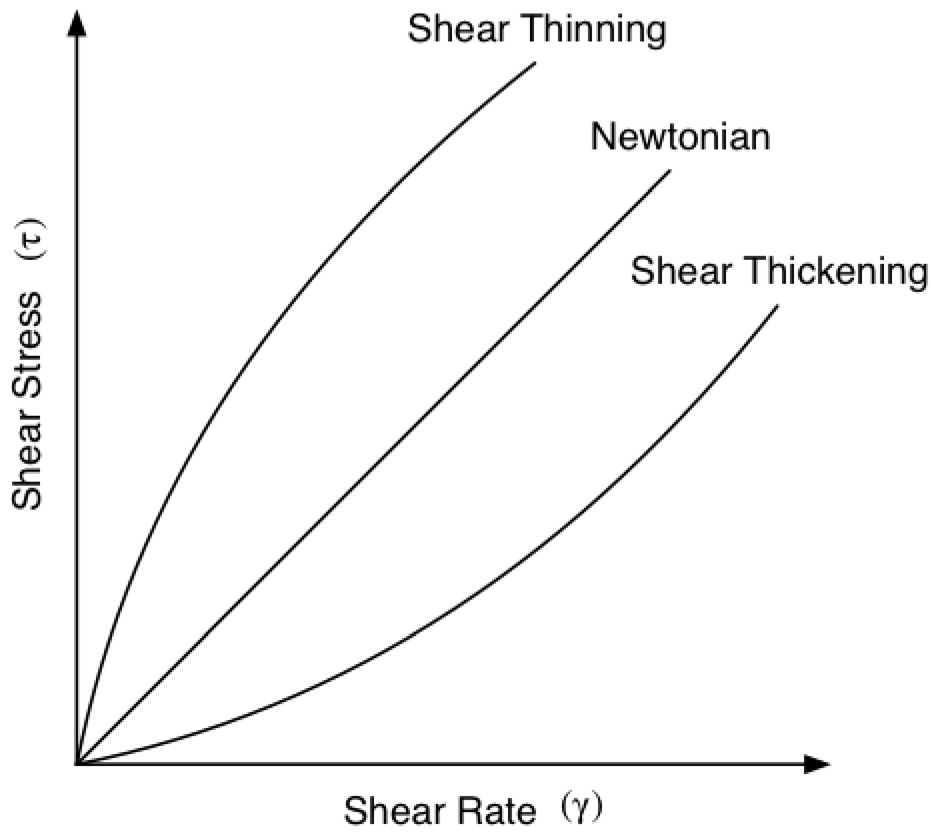

Figure 4: A stress-strain relationship for viscosity

Viscosity is a measure of a fluid's propensity to flow. There are two kinds of viscosity commonly reported, kinematic and dynamic. Dynamic viscosity is the relationship between the shear stress and the shear rate in a fluid. The Kinematic viscosity is the relationship between viscous and inertial forces in a fluid. Most common fluids are Newtonian fluids and their viscosity is constant with shear stress and shear rate. Non-Newtonian fluids are less common.

$$\tau = \mu \frac{du}{dy} \tag{2.11}$$

μ is the dynamic viscosity

2.3 Multiphase flow:

Multiphase flow as earlier described is a simultaneous flow of two or more phases in a pipe. As (Al-Safran & Brill, 2017) explains that “The significantly different densities and viscosities of these fluids make multiphase flow much more complicated than the single-phase flow calculations. Predicting multiphase-flow behavior in an oil and gas production system is further complicated by complex heat and mass transfer that takes place among hydrocarbon fluids as pressure and temperature change.

Despite the efforts made to understand and predict multiphase flow, to this date there is no single correlation or model that can be accurately applied to find the pressure gradient for all operational conditions. The parameters involved in the calculations are just too many and the best that can be done is to select the correlation or model that can give better predictions for specific operational conditions. It could be possible that, even for a given well, one correlation might be better for a given section of the production tubing but not for its entire length. (Hernandez, 2016)

{Carcaño-Silvan, 2021} explains that a good characteristic of the slug flow is the formation of gas bubbles that separate the liquid column into sections. These bubbles are called Taylor Bubbles (David and Taylor, 1950).

Multiphase flow which is a simultaneous flow of more than one phase become complicated when they are not dispersed evenly about the pipe length. This complexity affects the pressure drop, the flow rate, and of course the geometry relations which are of importance to pipe designers. The identification and prediction of multiphase flow patterns during transport processes is currently a challenge in the engineering industry as these flow patterns are fundamental to understanding the relationship between flow variables such as pressure and energy gradients. This in turn will help in the design, operation, and optimization of piping systems. **{Azzopardi, 2010}**

Due to the expansive variations experienced in multiphase flows, researchers have resorted to the concept of flow patterns of the fluid compositions in predicting models for pressure drop in pipes. For gas/liquid flows, the complications are caused by the interface between the phases giving rise to wide range of configurations in the channel with consequences both for the hydrodynamics and for heat and mass transfer. Accordingly, the following flow patterns have been identified in describing the configurations taken up by gas and liquid flowing together.

2.3.1 Flow patterns:

Bubbly flow: This is a phenomenon describing a continuous liquid phase with the gas phase dispersed as bubbles within it. These bubbles are formed at lower liquid velocities and travel with complex motion within the flow. With more formation of bubbles, coalescence may occur. For a horizontal flow however, unless at extremely high liquid velocities when the intensity of turbulence can disperse the bubbles about the cross section, gravity tends to make the bubbles accumulate at the top part of the pipe. This gives rise to a **Stratified flow** where the liquid remains at the lower part of the pipe land the gas above it. An increase in gas velocity will induce wavy form-like structures at the interface of the stratified flow to yield **Wavy flows**. (Taitel et. al 1980) formulated a relation for identifying a bubble flow, suggesting that at low gas and liquid rates, bubbly flow will most likely occur If this relation holds:

$$D > \sqrt{(\frac{\rho_l - \rho_g}{{\rho_l}^2})\sigma} \qquad (2.12)$$

Where D = diameter of the pipe, ρ_l = liquid density, ρ_g = gas density

σ = surface tension

2.3.2 Plug flow:

This flow pattern is otherwise known as slug flow. This occurs when coalescence begins i.e., at a certain gas rate and liquid holdup, the larger bubbles tend towards the channel, leaving the liquid as a slug. They are characteristically bullet-shaped and often called Taylor bubbles. Recently, it has been observed that this characteristic flow does not occur in larger-diameter pipes.

2.3.3 Churn flow:

"At higher velocities, the Taylor bubbles/liquid slugs in slug flow break down into unstable pattern in which there is an oscillatory motion of liquid in the tube**."{Azzopardi, 2010}.** This flow pattern is characteristic of high gas flow rates. The Plug and churn flow patterns are often grouped as intermittent flow as they both exhibit large fluctuations in void fraction and pressure drop.

2.3.4 Annular flow:

This type of flow occurs at certain flowrates where most of the liquid travel as drops, leading to the term mist flow.

Dispersed Bubble flow: fluid mixture that forms at high gas and liquid flow rates.

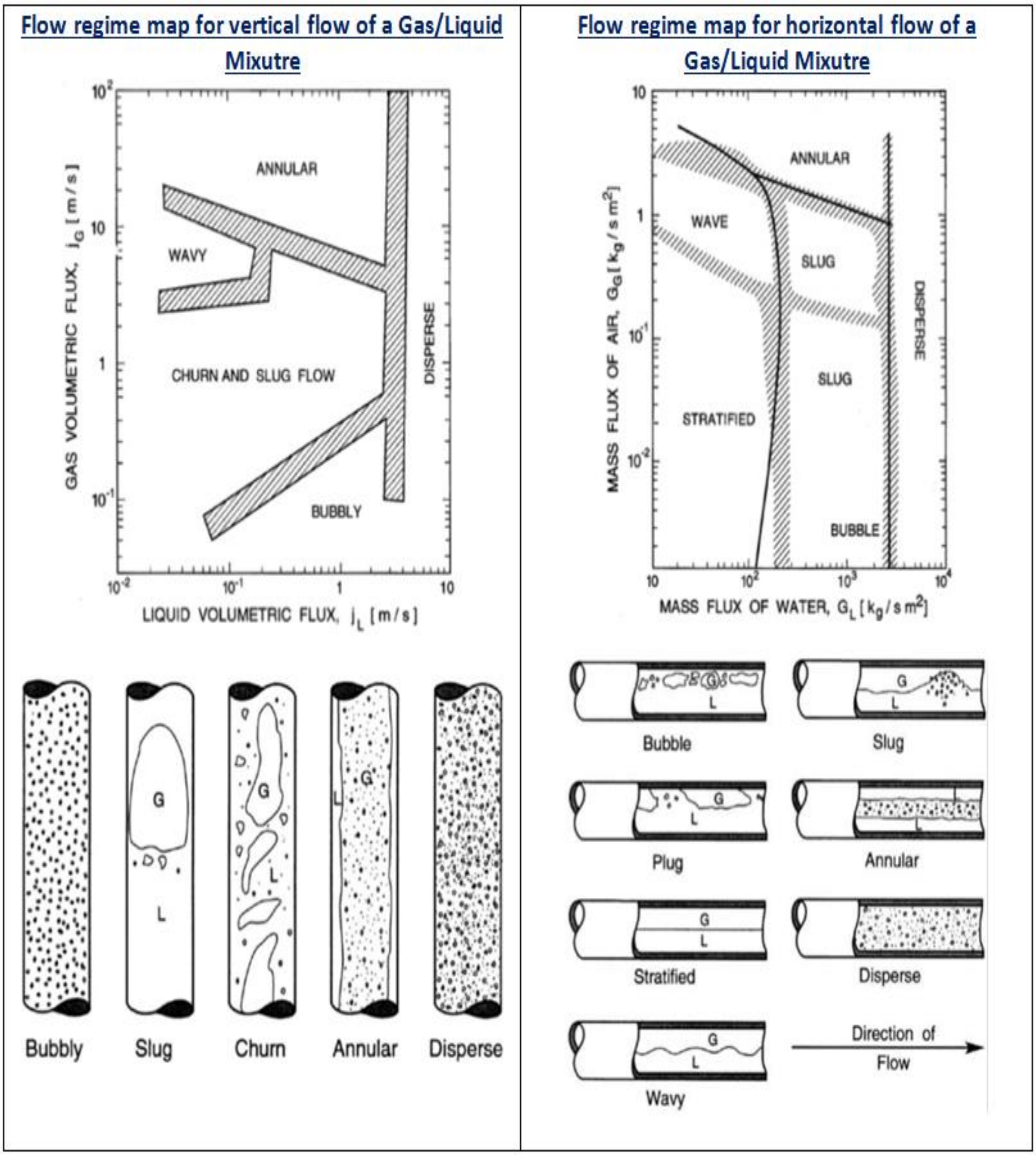

Figure 5: Flow regime diagram

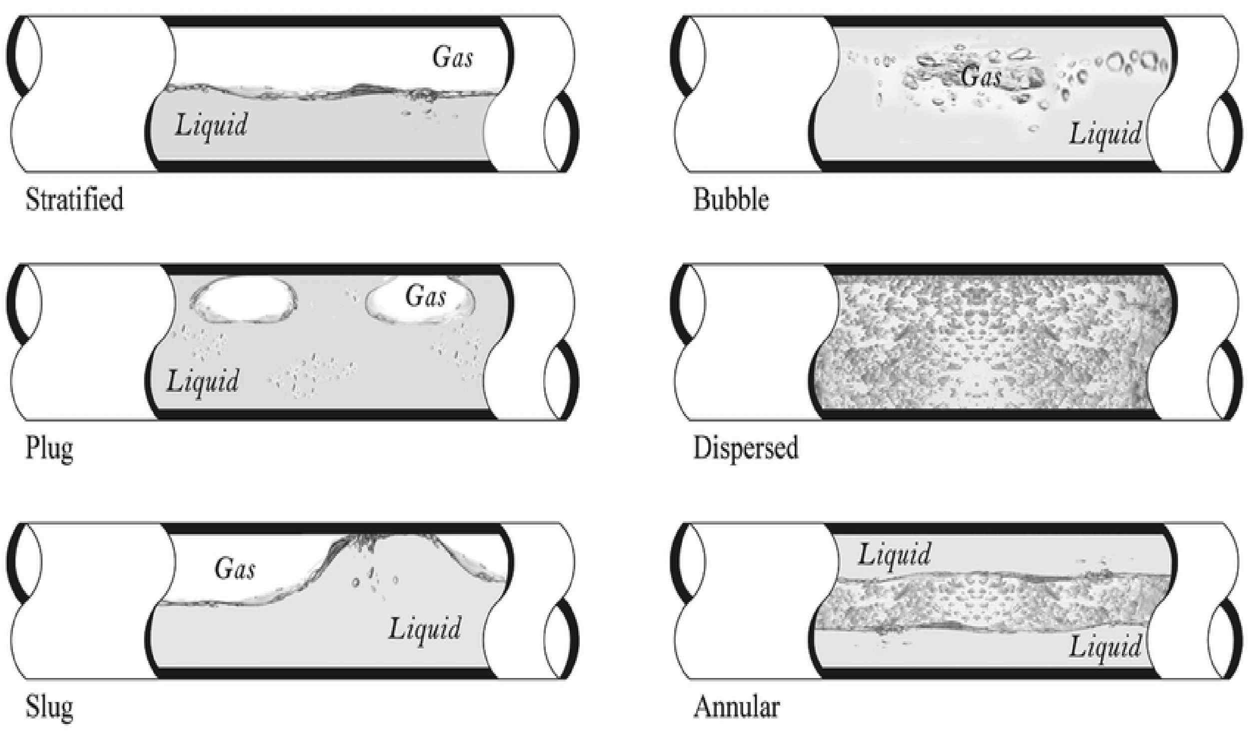

Figure 6: Horizontal flow regime diagram

2.4 Control Valves

Generally, it is the flow capability of a valve or choke at full open conditions. Valves are used to regulate the flow of fluid through a pipe. Prior, choke sizing has always been done using traditional methods of theory and experimentation employed by companies. These methods however can be inconvenient and costly if inaccurately done. Careful sizing of the choke or valve is necessary to prevent damage to the pipe through the effects of cavitation or flashing. Too small a valve could limit the required flow rate causing low recovery while an oversized valve can lead to instability in flow.

As discussed earlier, pressure losses in pipelines occur more in multiphase flows especially at the choke due to variations in the flow properties. The effect of losses is more prominent due to density differences. And this is why losses in the choke region must be considered a major loss.

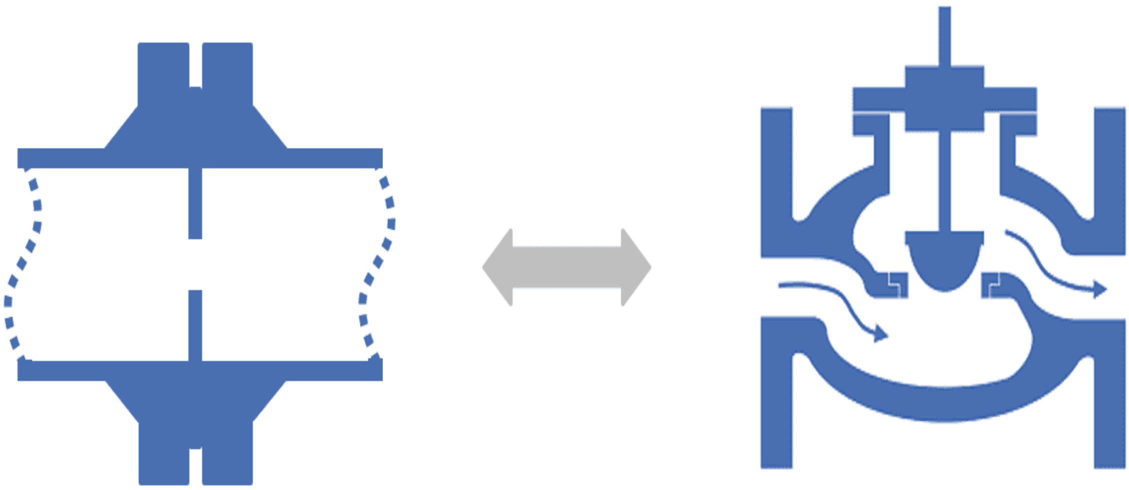

Figure 7: A representation of a choke system (https://neutrium.net/fluid-flow/pressure-loss-cv-and-kv-method/)

In recent times, standardized methods are being investigated as a guide when choosing valve sizing. Understanding the flow conditions around the choke in a pipeline can tremendously transform the uncertainties bothered around them. The effect could help maintain an actual flow rate of fluid flowing through while predicting flowing pressure losses as well.

Based on research, a commonly used method for valve sizing by companies can be traced to the principle of conservation, described by Daniel Bernoulli that the square of the fluid flow rate is directly proportional to the pressure differential and inversely proportional to the specific gravity of the fluid. Considering the energy losses due to friction and turbulence and varying discharge coefficients for various orifices, the basic sizing equation from which other parameters can also be obtained by substitutions has the following relation:

$$C_v = Q * \sqrt{\frac{S.G}{\Delta P}} \qquad (2.13)$$

Where: C_v = Control Valve sizing coefficient, ΔP = Pressure differential, Q= Flow rate (V*S)

$S.G$ = Specific gravity, S= Cross-sectional area, V= Velocity

The problem with this equation however is that it did not consider viscosity, an important fluid parameter.

To correct this error, there is an introduction of a correction factor F_v to make up for the viscosity effect, yielding:

$$C_{vr} = F_v * C_v \qquad (2.14)$$

$$Q = C_v * \sqrt{(\frac{\Delta P}{S.G})} \qquad (2.15)$$

A predicted pressure loss across the valve can be evaluated by back-calculation as thus:

$$\Delta P = S.G * (\frac{Q^2}{{C_{vr}}^2}) \qquad (2.16)$$

Where C_{vr}= corrected flow or sizing coefficient

{Singh, 2020} explains that the design requirements for valves handling for multiphase flow is different for single phase flows and is largely dependent on the flow regime within the valves. The changes in flow conditions during the operation of valves can have a huge effect on performance, especially in oil and gas applications where flow behaviors can rapidly change within the valve causing unwanted flow conditions. Therefore, recent practices in designing and sizing valves are based solely on global phase properties such as pressure drop of the bulk fluid across the valve and overall phase ratio.

Problems of cavitation and flashing can be managed when there is a good understanding of the valve flow conditions. However, due to the limited information about the local flow field within the valve internal parts, valves are only designed according to global performance indicators and variables which do not take into account local flow conditions, as with multiphase fluids, the flow behaviour across the valve becomes more complex. Numerous investigations have been done by (Kang et al 2006, Yang et. al 2011) to understand the flow features within valves in order to link design methodologies with the local features to avoid problems of cavitation and flashing.

2.4.1 Flashing and Cavitation

These are phenomena in valve sizing procedures that can limit flow tremendously if not properly accounted for. They are also responsible for structural damage to valves through erosion. A good understanding of the happenings in a valve can reduce the undesirable effects of flashing or cavitation, allowing a good prediction of pressure in that area as well as sustaining a high-flowing pressure recovery to the delivery point.

To keep a high flow rate through the valve, it is necessary to have a high-velocity head, which is often followed by a pressure drop at the opening of the valve. Further downstream, as the fluid expands, the velocity or kinetic energy of the fluid drops and the pressure normalizes. The pressure after going through the valve orifice however does not equal the pressure that existed upstream of the valve. The pressure differential ΔP that exists across the valve is a measure of the amount of energy that was dissipated in the valve. This pressure differential as the fluid flows through the choke is the primary concern of the research.

The underlying concept that describes the pressure differential across the choke occurs between the inlet valve and the orifice. As fluid passes through the valve, if the pressure drop due to an increased flow velocity, is less than the vapor pressure of the fluid, bubbles will form. A further decrease will create more bubbles. At the valve outlet, the bubbles will remain if the flowing pressure remains below the vapor pressure. This process is called flashing, which could create serious problems to valve trim parts. If the outlet pressure is sufficiently higher than the vapor pressure, the bubbles will collapse, producing cavitation. Cavitation wears material surface. It reduces efficiency or lead to loss of process control resulting from effects of unacceptable vibrations from cavitations.

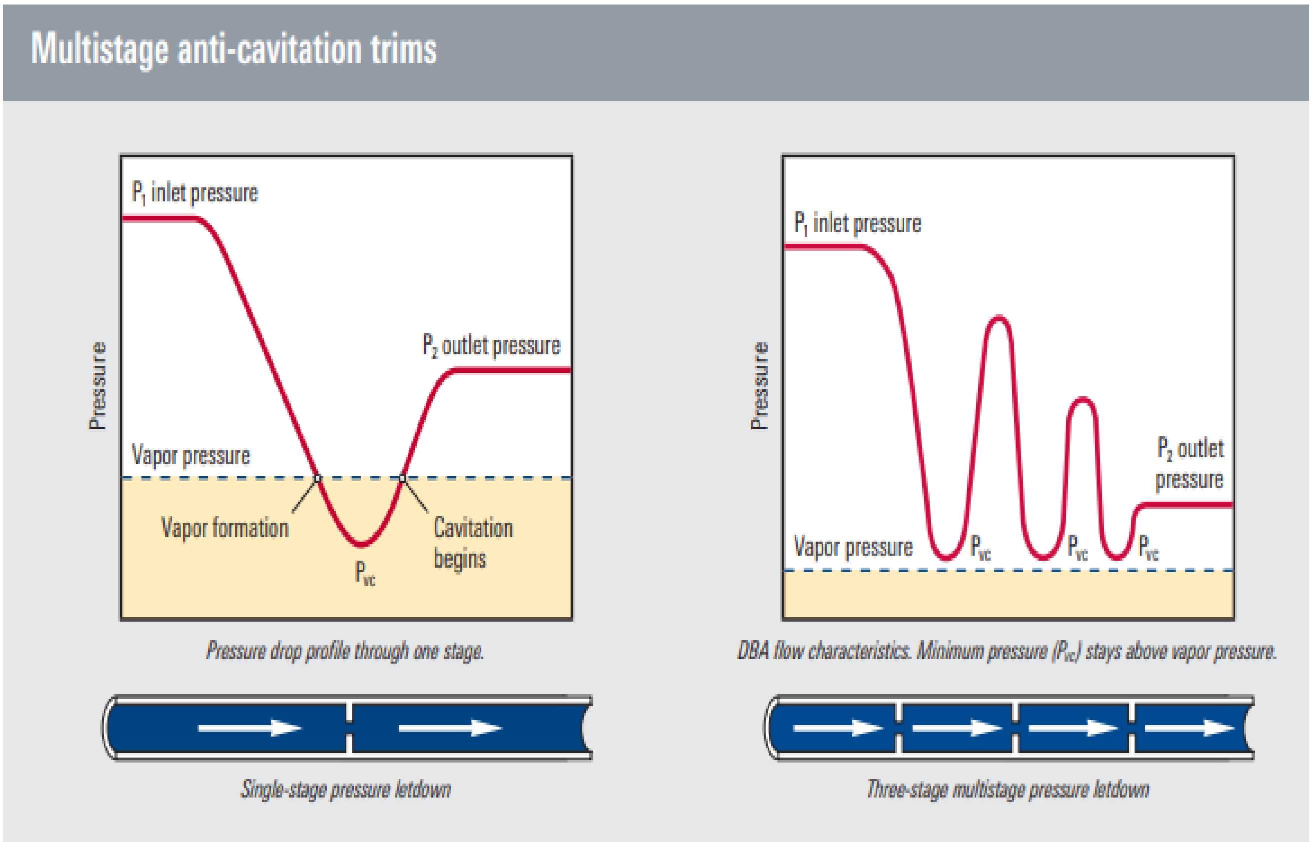

Figure 8: An illustration of flowing pressure drops through a choke.

Knowing the maximum allowable mass flowrate through a valve system is essential to production control in the oil and gas industry. If the variations in pressure and temperature conditions across a choke can be correlated with the mass flowrate, control valve coefficient, and other properties of the flowing fluid, this may contribute to determining any of the mentioned parameters in a simple yet less costly form when compared to other designs. **{Schüller, 2003}**

2.4.2 Choked Flow

A choked flow exists when there is a continual formation of bubbles resulting from an increased velocity flow at the entrance of the valve. An increased pressure drop will increase bubbles which would create a crowding situation that tends to obstruct flow, hence termed a choked flow. It is important to know that a further increase in pressure drop after a choked condition is attained, will not produce an increased flow.

2.4.3 Non-Choked flow:

This a kind of flow where the Mach number is either less than one or equal to one.

2.5 Literature reviews

A quick review of models in use for evaluating flow patterns and pressure loss in pipes and across chokes for multiphase flows.

(**Ansari & Sylvester, 1988)** formulated a mechanistic model for a two-phase flow in a vertical pipe that allows calculation of liquid holdup and pressure drop. The model was formulated on the assumptions that the flow is fully developed and stable. It also assumes that the gas is discretely and uniformly dispersed as bubbles in the liquid phase. On evaluation by comparison with field data obtained from Tulsa University Fluid Flow Projects (TUFFP) data bank, the model was observed to predict the pressure drop reasonably well with an average deviation of -2.1%. The deviation indicates that the model underpredicted the pressure drop by assuming that bubble flow existed over the entire pipe length. However, in comparison with five commonly used empirical correlations like those of Duns and Ros (1963), Hagedorn and Brown (1965), Beggs and Brill (1973), Orkiszewski (1967), and Mukerjee and Brill (1985), it was discovered that the model outperforms each of the correlations, showing a lower absolute average difference and a lower standard deviation.

Yu et al. (2009) presented a mechanistic model to predict the flow pattern, the liquid holdup, and the pressure gradient for multiphase flow in annular ducts. The models used for flow pattern transitions were the unified model developed by Zhang et al. (2003a) for dispersed bubble and annular flow, Caetano (1985) for the bubble-flow transition, and the modified model of Kaya et al. (2001) for the transition from slug to churn flow. The churn-flow model was based on the modified model developed by Zhang et al. (2003b) for circular pipes.

(Hernandez, 2016) summarizes that **"**There are many calculation procedures that can be used to find the pressure distribution along the production tubing. These procedures can be categorized as follows: Empirical correlations that assume homogeneous flow and do not take into consideration the flow pattern. These were the first correlations used in the oil industry and they are seldom used today because they do not give precise results. An example of this type of correlation is the Poettmann and Carpenter (1952). Empirical correlations that do not consider the flow pattern in their calculation procedures but do consider the fact that the phases can travel at different velocities and therefore the estimation of the liquid holdup plays a vital role. This is the case of the Hagedorn and Brown correlation (1965). Empirical correlations that have different calculation procedures for each flow pattern. They take into consideration the fact that for most flow patterns, but not for all, the phases can travel at different velocities. Examples of this type of correlation, among many others, are the Orkiszewski correlation (1967) for vertical flow, and the Beggs and Brill correlation (1973) for any pipe inclination angle. Mechanistic models use the hydrodynamic behavior of each flow pattern to develop calculation procedures based on mass and momentum-balance equations, as well as on many closures."

"Numerous TPR models have been developed for analyzing multiphase flow in vertical pipes. **Brown (1977)** presents a thorough review of these models. The models for multiphase flow wells fall into two categories: (1) homogeneous-flow models and (2) separated-flow models. Homogeneous models treat multiphase flow as a homogeneous mixture and do not consider the effects of liquid holdup (no-slip assumption). Therefore, these models are less accurate and are usually calibrated with local operating conditions in field applications. The major advantage of these models comes from their mechanistic nature. They can manage gas-oil-water three-phase and gas-oil-water-sand four-phase systems. It is easy to code these mechanistic models in computer programs."

Lockhart Martinelli model considers each phase to be flowing separately in the channel, each occupying a given fraction of the pipe's section and each with its velocity. It is adequate for two-phase flows at low and moderate pressures. For applications at higher pressures, the revised models of Martinelli and Nelson (1948) and Thom (1964) are recommended. The model makes use of a multiplier for the liquid and gas phases.

The single-phase friction factors of the liquid and the vapor are based on the single phase flowing alone in the channel, in either viscous laminar (v) or turbulent (t) regimes.
Δp_l can be calculated classically but with the application of $(1-x)^2$ in the expression and Δp_g with the application of vapor quality x^2 respectively. **C** is a factor of the flow regime.

{Beggs, 1973} modelled flows for two-phase flows in inclined, vertical, and horizontal pipes. But there were assumptions of no slip which is only applicable in flow regimes where liquid and gas velocities are the same. Pipe relative roughness was included which makes it a suitable model for evaluating losses.

Orkiszewski (1967), took existing correlations and compared them to field results. Selected the best correlations for different regimes and developed a single correlation. Although it is a famous flow model for evaluating multiphase fluids, it may show discontinuities when crossing regime boundaries.

{Singh, 2020} investigated a validated CFD model to locally and globally quantify the performance characteristics of a severe-service valve handling multiphase gas and liquid flow. Their statement problem was to validate the model with benchmark experiments by incorporating the limitations of the flow conditions within the valve. Two valve opening positions were considered with different inlet volume conditions to simulate real life situations. The results obtained showed some non-uniformity in the local air, water and void fraction distributions within the valve. The phase velocity and void fraction data obtained from the validated CFD model were used to obtain relationships for local void fraction distribution and flow coefficient. The investigation done thus allows for local flow characteristic determination and is incorporated in sizing methodology for severe-service control valve system for multiphase flows. Some of the equations cited in the determination of the flow coefficient for multiphase flow are:

$$\rho_{mix} = \alpha_{inlet} * \rho_{gas} + (1 - \alpha_{inlet})\rho_{water} \tag{2.17}$$

$$K_v = 11.56 Q_{mix} \sqrt{\frac{S.G}{\Delta P}} \tag{2.18}$$

$$S.G = \frac{\rho_{mix}}{\rho_{water}} \tag{2.19}$$

K_v *is the flow coefficient*

The assumptions by {Diener, 2005} who formulated the model lies on the premise that the fluids are well mixed or homogenous and travel at the same velocity, hence no slippage**.**

Chapter 3

3.1 METHODOLOGY

Several models can be used to predict the pressure loss of multiphase flow through a pipe. One popular method employed is the homogenous model, which assumes that the phases are well-mixed and behave as a single phase. Another method is the drift-flux model, which considers the segregation of the phases and the heat and mass transfer between them.

This thesis, as earlier explained, will use a combination of both quantitative and qualitative methods, as measured data from OneSubsea company will be used to evaluate Bernoulli equation for flows through a valve system that can help predict to a measurable accuracy the pressure loss of multiphase flow through a recirculation pipe, with emphasis at the choke.

3.2 Models of Data Analysis

Any of the models described in the literature review can be employed to predict our pressure profile for the recirculation line depending on the data provided by OneSubsea.

A mechanistic homogenous model will be useful in evaluating the pressure loss across the pipe. This model is cited because the data obtained assumes that the fluids are homogenous, hence same flow rates across the choke area. Following the Bernoulli equation, the total pressure loss through a line is a combination of frictional losses, and losses at the components. The limitation to this homogenous model however is in the negligence of slippage or liquid holdup.

The empirical data obtained are not assessed data from laboratory tests but from field measurements. As such, there might be limitations to parameters needed to evaluate the pressure loss using the mechanistic model.

$$\text{Total } \Delta Pl = \Delta p \text{ friction} + \Delta p \text{ bend} + \Delta p \text{ choke}$$

$$\Delta Pl, \text{total} = \sum \Delta Pl, f + \sum \Delta Pl, c$$

$$\Delta Pl, c = \sum \Delta Pl, \text{bend} + \sum \Delta Pl, \text{choke}$$

$$\Delta Pb, \text{total} = \sum K.\frac{\overline{V}^2}{2g} \text{ (bend)}$$

$$\Delta Pl\text{choke} = \sum \Delta Pl, \text{total} - \sum \Delta Pl, f - \sum \Delta Pl, \text{bend}$$

3.2.1 Method 1:

The process for obtaining the pressure drop across the choke is enumerated thus:

Step 1**:** Pressure drop across the entire pipe has been provided in the empirical data.

Step 2: Obtain the frictional losses through pipe using mechanistic model.

Step 3: Obtain the minor loss from the bend.

Step 4: Obtain loss at the choke by subtracting the other losses from the total pressure loss through the recirculation line.

3.2.2 Method 2:

Step 1: Fluid flowing conditions are obtained for every stem travel as the fluid recirculates through the pipe.

Step 1: Obtain the bulk density for gas from the GVF. (GVF * Gas Density)

Step 2: Obtain the bulk density for each liquid phase (oil and water) from the water-liquid-ratio WLR.

Step 3: Obtain the liquid density mix for both oil and water.

Step 4: Obtain the bulk density for liquid phase from the GVF.

Step 5: Obtain the total density mixture from the gas and liquid phase densities.

Step 6: Obtain Cv by linear interpolation.

Step 7: Obtain the Specific gravity (S.G) of the fluid mixture.

Step 8: Obtain the pressure drop across the choke and compare with the mechanistic homogenous model.

Step 9: Plot a graph of flowrate 'Q' against dP.

Step 10: Plot a graph of GVF against dP.

From equation (2.17), the relation for oil-water-gas flow was obtained.

$$\rho_{mix} = \alpha_{inlet} * \rho_{gas} + (1 - \alpha_{inlet})\rho_{water} \tag{2.17}$$

Equally:

$$\rho_{mix} = \alpha_{inlet} * \rho_{gas} + (1 - \alpha_{inlet})\rho_{liquid\ mix} \tag{2.20}$$

$$\rho_{liquid\ mix} = WLR * \rho_{water} + (1 - WLR)\rho_O \tag{2.21}$$

$$S.G = \frac{\rho_{mix}}{\rho_{water}} \tag{2.22}$$

From equation 2.13,

$$C_v = Q * \sqrt{\frac{S.G}{\Delta P}}$$

$$\Delta P = S.G * (\frac{Q^2}{C_v^2})$$

Where Q is measured in US gallon per min and ΔP is in psi

Also: $\Delta P = S.G * \left(\frac{Q^2}{K_v^2}\right),\ where\ K_v = 0.8646\ C_v$

For K_v, ΔP is measured in bar and Q is in $\frac{m^3}{hr}$

By substitution, $\Delta P = S.G * (\frac{Q^2}{C_v^2})[1.33773]$

$\alpha_{inlet} = void\ fraction$

Chapter 4

4.1 RESULTS

The graph represented below is that of the fluid flow rate against the pressure drop. The pressure drop here was obtained from the inlet fluid properties only using the steps described in the methodology.

The obtained results show a good correlation with the continuity equation where an increase in flow rate across an opening will result in an increased pressure drop across the system. A reduced valve opening will induce an increased velocity, hence an increase in flow rate and an increase in pressure drop. The dips observed at some points could be referred to the effects of the flow regime or composition.

Continuity equation:

Mass flow in = mass flow out

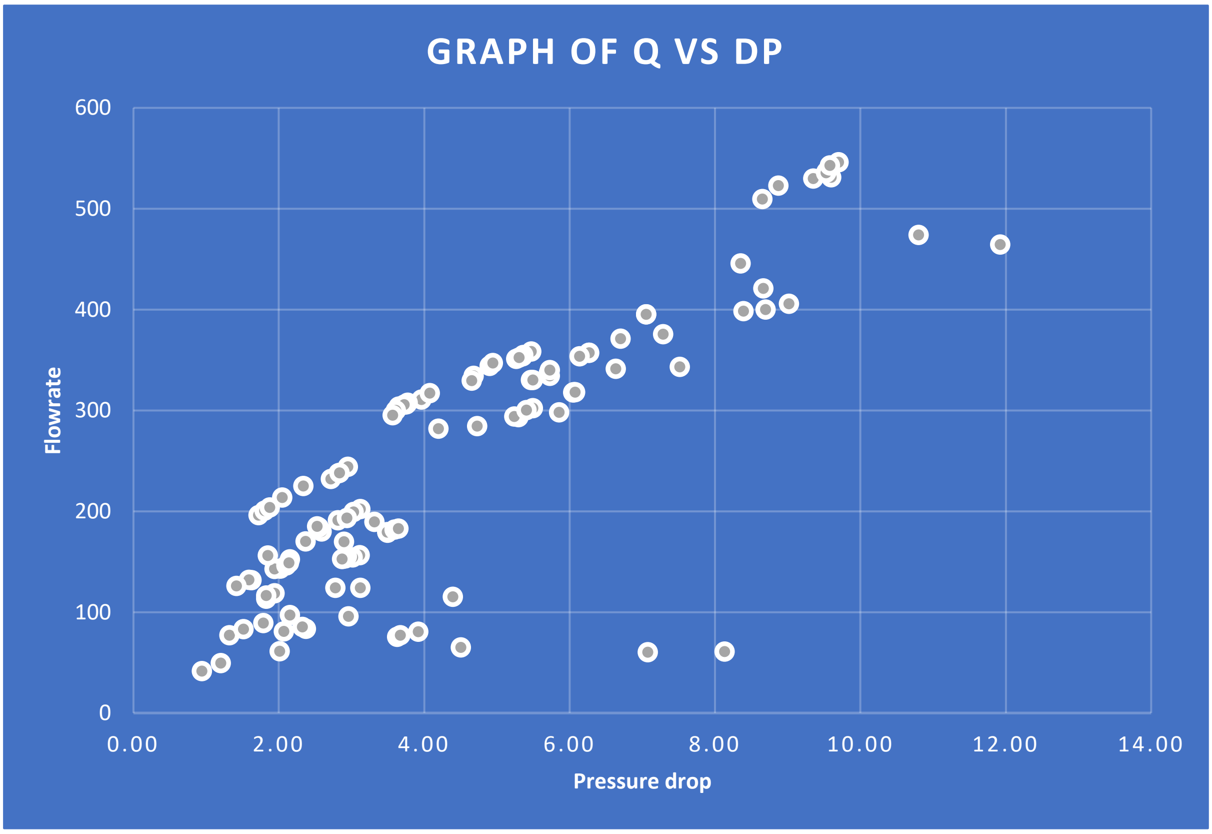

Figure 9: A graphical illustration of flowrate against dP

Here, the average inlet and outlet density mixtures were used in the determination of pressure drop across the valve which is then evaluated against the flowrate. As can be observed, there is a good similarity in both graphical representations indicating a good correlation.

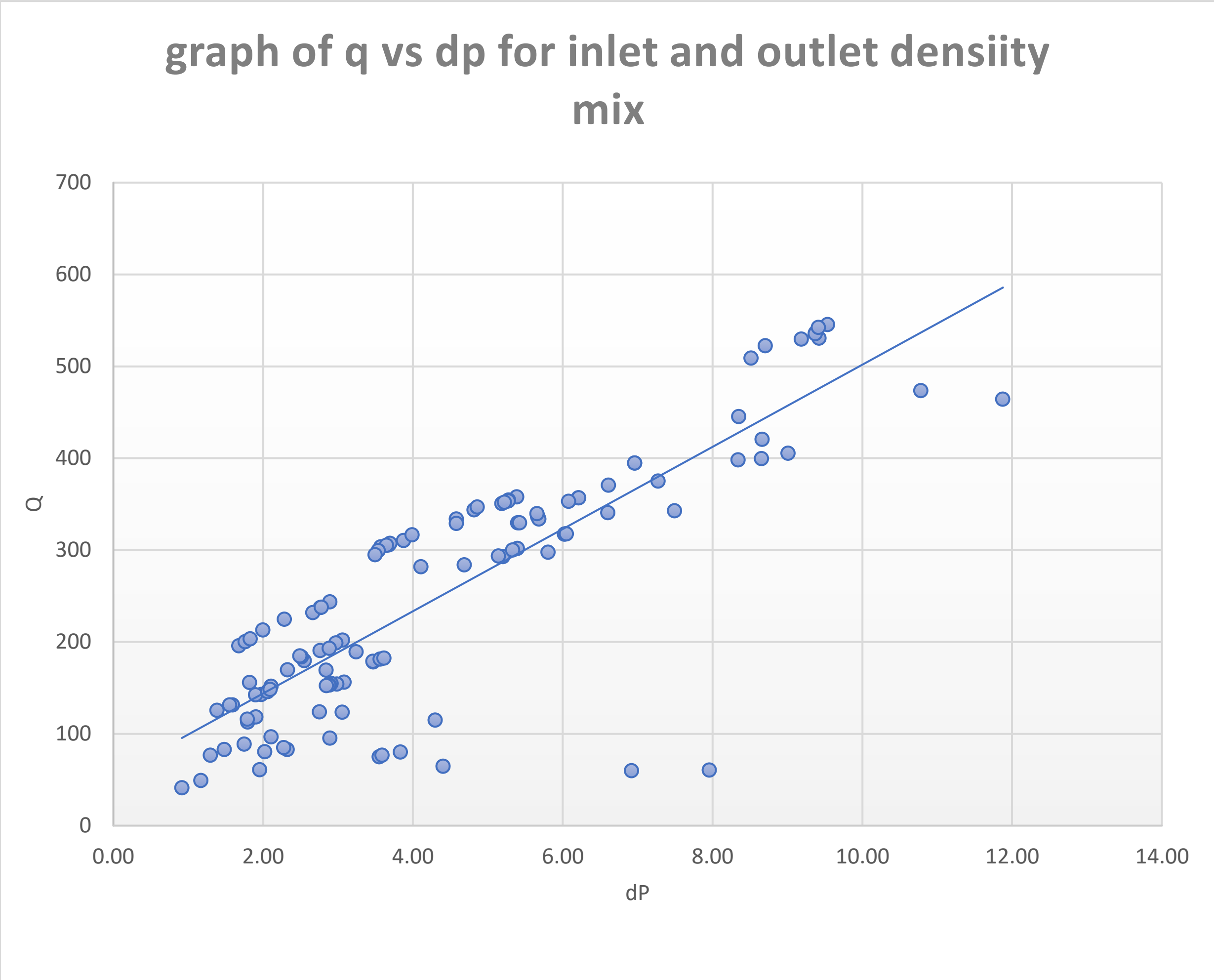

Figure 10: A representation of Q VS Pressure drop for avg. inlet and outlet density mixture.

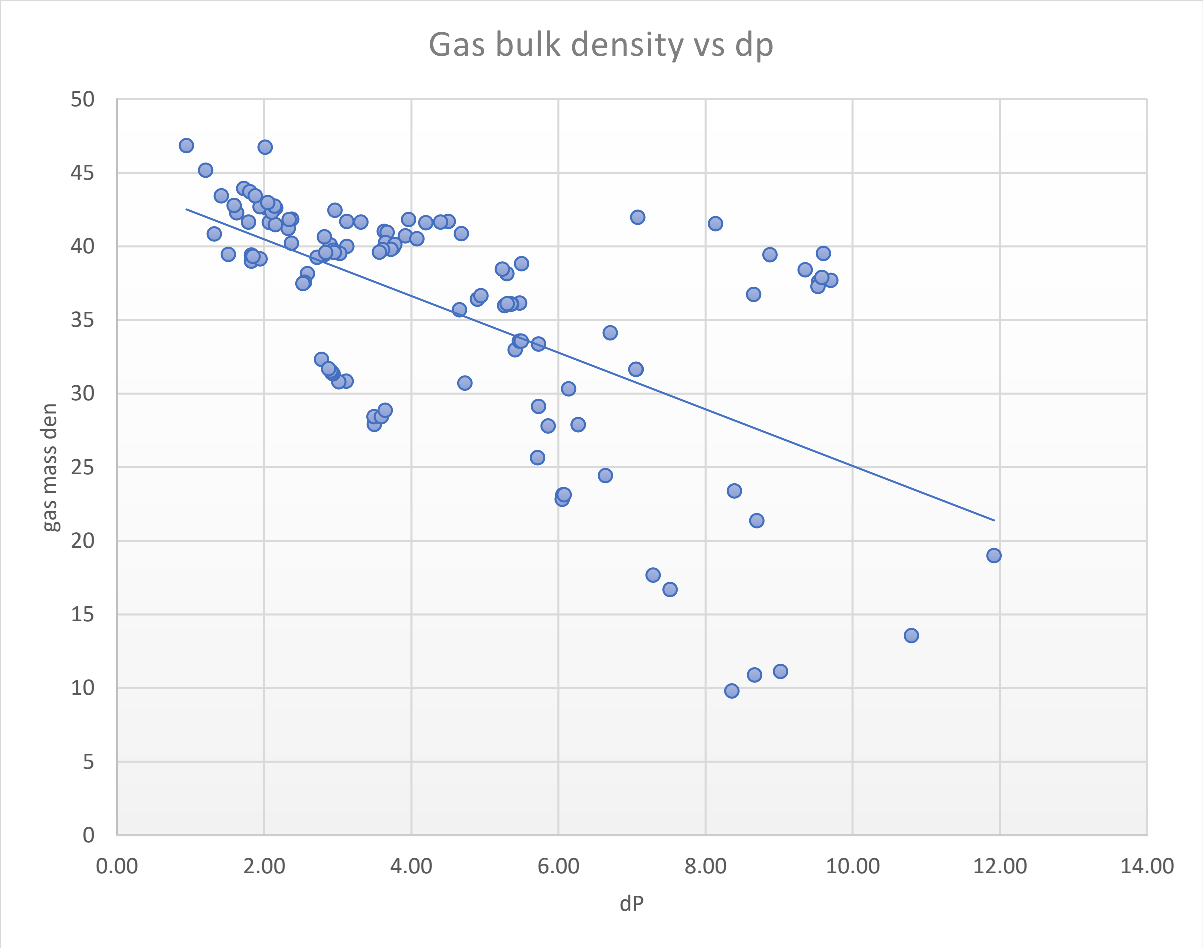

Figure 11: A representation of gas bulk density against dP

This result illustrates the effect of the gas volume fraction GVF in the fluid mixture on the pressure drop across the choke. There is an observable trendline showing results of increased pressure drop after a certain period. The result of the scattered wavelength is a result of the constant changes that the GVF undergoes from time to time due to changes in temperature.

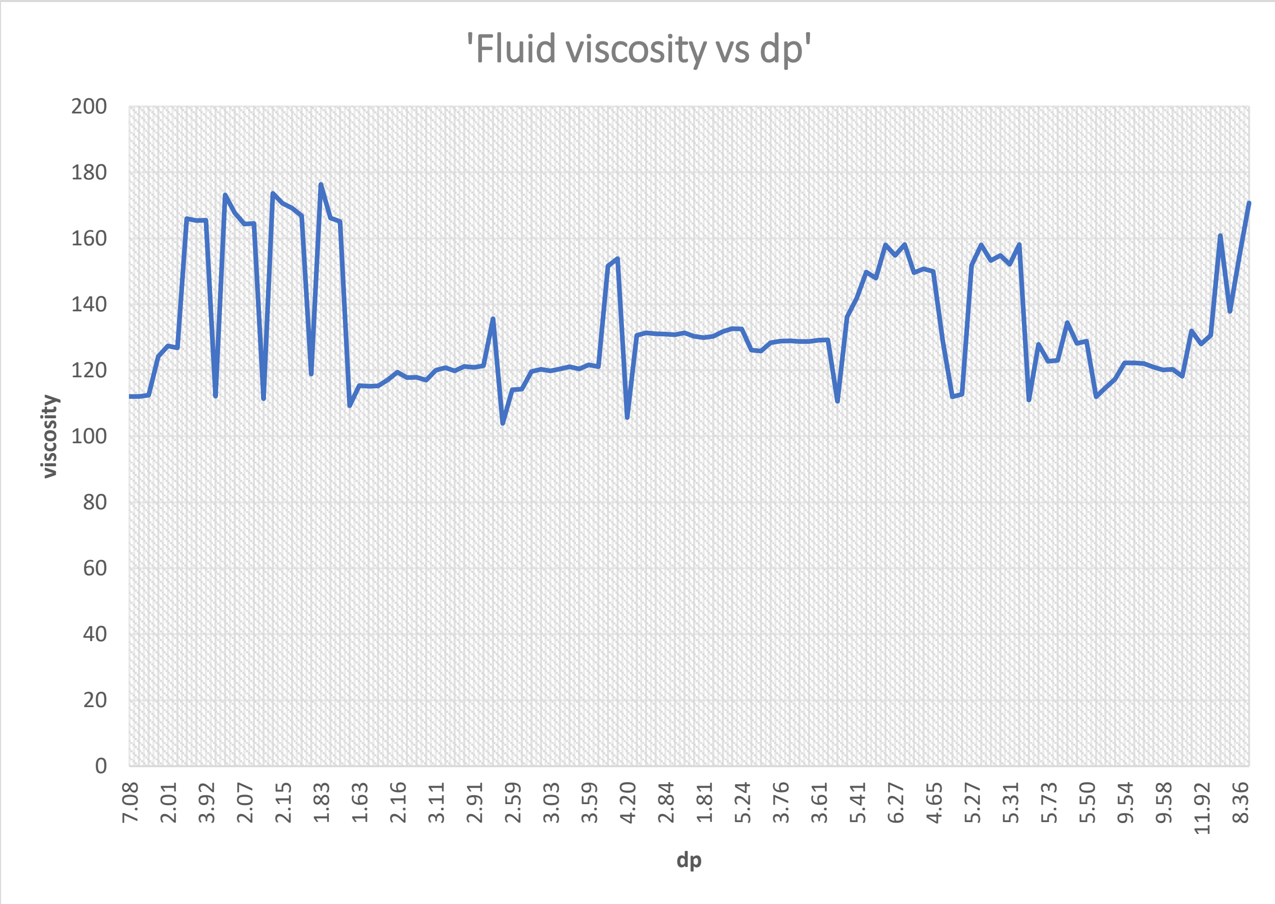

Figure 12: An illustration of fluid viscosity vs dP

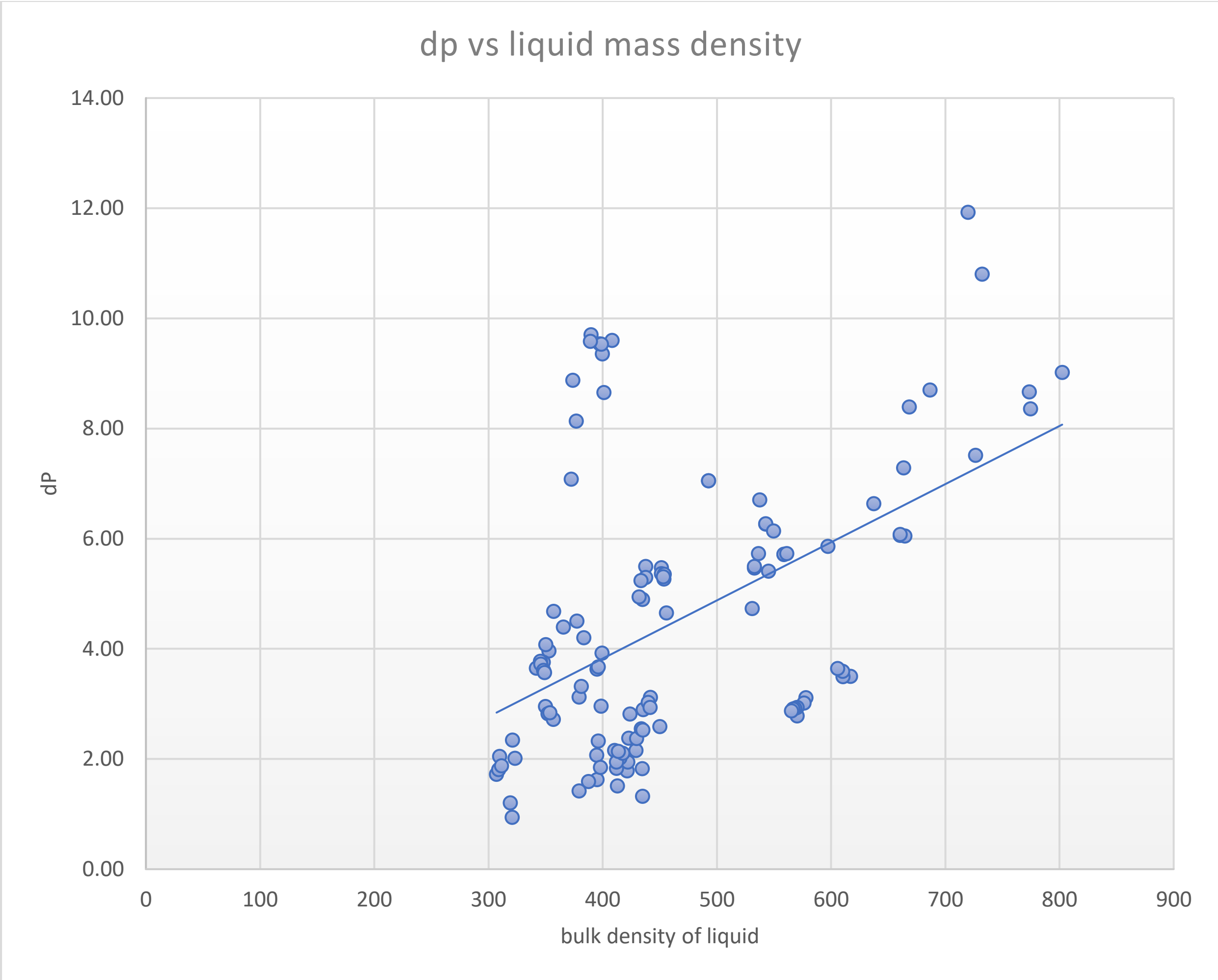

Figure 13: Graph of liquid bulk density against obtained pressure drop.

This is also an upward trend. The wide density difference between the liquid and gas phases will induce a slip loss, although we assume that the flow is highly homogenous.

Chapter 5

5.1 DISCUSSION

Pressure loss across valves is just as important as frictional losses in a straight pipe. The pressure drop for multiphase flows generally is complex problem at the choke due to variations in densities and flow regimes of the phases involved. This has resulted in the inability to predictably identify the losses within the valve, hence the inability to design valving systems efficiently. Effects of inaccurate predictions could create damages to piping systems from vibrations and noises to wearing of materials through cavitations and flashing. A good prediction of pressure drops could also prevent excess pump energy for recirculation of flows. This study therefore aimed at understanding the flow characteristics in recirculation pipes and across a choke to predict the pressure drops that occur within the choke and compared to the overall loss.

From the empirical data provided, pressure drop values were obtained using Bernoulli equation for multiphase flows (Oil, water, and gas) through a control valve. The results obtained when evaluated against the fluids characteristics indicate a good correlation with continuity equation and as described in the theoretical analysis.

The pressure drop was evaluated against the liquid flow rate, and there was an upward trend showing that an increased flowrate will lead to an increased pressure drop across the choke. Quantitative relationships were also determined between GVF, Bulk densities, viscosities and the pressure drop to see the resulting effects on the overall loss. As shown in the result section, an increase in any of these other parameters will cause a drop in pressure.

The knowledge from the flowrate plot against the predicted pressure can be used to identify the maximum allowable pressure drop and flow rate to prevent cavitation or flashing effects.

The model suggests to a certain degree that the pressure drop across a choke or in a valve can be predicted with some measure of error. The error resulting from the assumption that the flow is entirely homogenous.

For this data, the results obtained follow an agreed trend that is satisfactory for the calculation of pressure drops across chokes for multiphase flows (oil-water-gas).

Chapter 6

6.1 CONCLUSION AND RECOMMENDATION

This research aimed at predicting pressure loss across a choke through a recirculation pipe for multiphase flow. Based on quantitative and qualitative analysis of data provided by OneSubsea, it can be concluded that the flowrate which is a function of the control valve and density variations are two major parameters to consider when designing valve systems. The results indicate that there is an increased pressure drop at high flow rates.

Although the pressure drop computed for the 3-phase flow shows a positive insight for designing valve systems, there are limitations however to the model used.

The model assumes a homogenous flow of the phases, thereby ruling out any case of slip loss within the system. Further research is therefore required to establish the flow regimes of the individual phases identified and incorporated into the model for higher accuracy of pressure drop prediction across the choke.

Obtained pressure losses from this process can help regulate the required flowrate across a choke and to also understand the effects of the other relationships established in the result section.

REFERENCES

Al-Safran, E. M., & Brill, J. P. (2017). Applied multiphase flow in pipes and flow assurance: oil and gas production. Society of Petroleum Engineers Richardson, Texas, USA.

Ansari, A., & Sylvester, N. (1988). A mechanistic model for two-phase bubble flow in vertical pipes. AIChE journal, 34(8), 1392-1394.

Brill, J. P. (2010). Modeling multiphase flow in pipes. The Way Ahead, 6(02), 16-17.

Fancher, G. H., & Brown, K. E. (1962). Prediction of pressure gradients for multiphase flow in tubing. Fall Meeting of the Society of Petroleum Engineers of AIME,

Griffith, P. (1984). Multiphase flow in pipes. Journal of Petroleum technology, 36(03), 361-367.

Hernandez, A. (2016). Fundamentals of gas lift engineering: Well design and troubleshooting. Gulf Professional Publishing.

Khaleefa Ali, S. (2019). Study of Pressure Losses in Piping System. https://doi.org/10.21275/ART20198900

Tec-Science. (2020). Pressure loss in pipe systems (Darcy friction factor).

Xu, J. y., Gao, M. c., & Zhang, J. (2014). Pressure Drop Models for Gas/Non-Newtonian Power-Law Fluids Flow in Horizontal Pipes. Chemical Engineering & Technology, 37(4), 717-722.

Carcaño-Silvan, C., Soto-Cortes, G., & Rivera-Trejo, F. (2021). Characterization of slug flow in heavy oil and gas mixtures. *Revista Mexicana de Ingeniería Química*, *20*(1), 1-12.

Singh, D., Aliyu, A., Charlton, M., Mishra, R., Asim, T., & Oliveira, A. (2020). Local multiphase flow characteristics of a severe-service control valve. *Journal of Petroleum Science and Engineering*, *195*, 107557.

Oliveira, B. R., Leal, B. C., Pereira, L., Borges, R. F. D., Paraiso, E. D. H., Magalhaes, S. D., Rocha, J. M., Calcada, L. A., & Scheid, C. M. (2021). A model to calculate the pressure loss of Newtonian and non-Newtonian fluids flow in coiled tubing operations. *Journal of Petroleum Science and Engineering*, *204*. https://doi.org/ARTN 10864010.1016/j.petrol.2021.108640

Beggs, D. H., & Brill, J. P. (1973). A study of two-phase flow in inclined pipes. *Journal of Petroleum technology*, *25*(05), 607-617.

Spedding, P., Bénard, E., & McNally, G. (2005). Two-and Three-Phase Flow Through a 90 Degree Bend. *Developments in Chemical Engineering and Mineral Processing*, *13*(5-6), 719-730.

EN, B. (2003). Industrial-process Control Valves. Part 2-5: Flow Capacity-Sizing Equations for Fluid Flow through Multistage Control Valves with Interstage Recovery.

Fancher, G. H., & Brown, K. E. (1962). Prediction of pressure gradients for multiphase flow in tubing. Fall Meeting of the Society of Petroleum Engineers of AIME, Schüller, R., Solbakken, T., & Selmer-Olsen, S. (2003). Evaluation of multiphase flow rate models for chokes under subcritical oil/gas/water flow conditions. *SPE production & facilities*, *18*(03), 170-181.

Azzopardi, B. (2010). Multiphase flow. *Chemical Engineering and Chemical Process Technology-Volume I: Fundamentals of Chemical Engineering*, 97.

Kang, S., Yoon, J., Kang, S., & Lee, B. (2006). Numerical and experimental investigation on backward fitting effect on valve flow coefficient. *Proceedings of the Institution of Mechanical Engineers, Part E: Journal of Process Mechanical Engineering*, *220*(4), 217-220.

Diener, R., & Schmidt, J. (2005). Sizing of throttling device for gas/liquid two-phase flow part 2: Control valves, orifices, and nozzles. *Process Safety Progress*, *24*(1), 29-37.

https://neutrium.net/fluid-flow/pressure-loss-cv-and-kv-method/

Sheldon, C., & Schuder, C. (1965). Sizing control valves for liquid-gas mixtures. *Instruments and Control Systems*, *38*, 134-136.

APPENDICES

Appendix A: Flow characteristics of the control valve

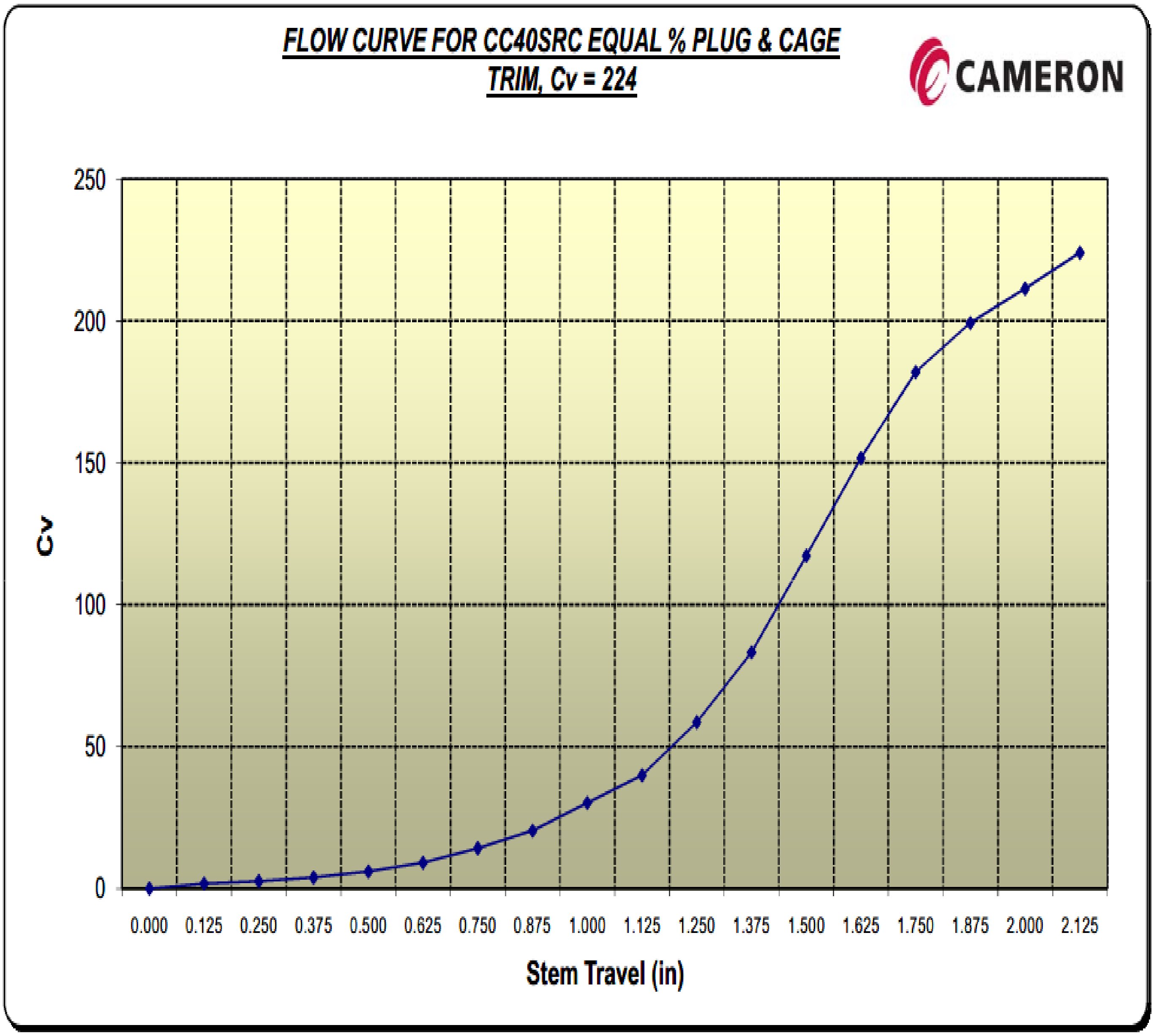

Cv	0	1.8	2.57	3.9	6	9.1	14.2	20.4	30.2	39.9	58.6	83.2	117.2	151.7	182	199.3	211.3	224
% Travel	0	6	12	18	24	29	35	41	47	53	59	65	71	76	82	88	94	100
Travel	0	0.125	0.25	0.375	0.5	0.625	0.75	0.875	1	1.125	1.25	1.375	1.5	1.625	1.75	1.875	2	2.125
% Open	0.0	0.8	1.1	1.7	2.7	4.1	6.3	9.1	13.5	17.8	26.2	37.1	52.3	67.7	81.3	89.0	94.3	100.0

Appendix B: Flow Characteristics for pressure drop formulation

	Process conditions					Density [kg/m3]						Ratios [%]				
	Inlet		Outlet			Inlet conditions			Outlet conditions					Viscosity [cP]	Choke position [%]	Total flow [Am3/h]
Flow period	Pressure [bar]	Temp. [C]	Pressure [bar]	Temperature [C]	dP [bar]	Oil	Water	Gas	Oil	Water	Gas	WLR	GVF			
1	103.9	53.3	46.9	44.8	56.9	888.1	1002.8	69.4	907.6	1005.2	31.1	46.5	60.4	112.0	7.5	60.1
2	103.6	53.2	46.9	44.8	56.7	888.3	1002.8	69.3	907.7	1005.2	31.1	45.9	59.9	112.0	7.1	60.5
3	104.0	53.2	47.0	44.7	57.1	888.2	1002.8	69.6	907.7	1005.2	31.1	47.3	59.9	112.4	10.2	64.8
4	103.8	56.0	48.0	46.8	55.8	886.7	1001.9	68.5	906.3	1004.6	31.5	43.2	65.9	124.2	14.0	49.2
5	107.5	55.2	48.0	45.9	59.5	886.3	1002.2	71.4	906.8	1004.8	31.7	43.1	65.5	127.4	13.5	60.9
6	107.5	55.4	48.0	46.0	59.5	886.1	1002.1	71.3	906.7	1004.8	31.7	43.0	65.7	126.8	13.3	41.3
7	108.2	58.6	45.0	51.9	63.2	884.2	1001.1	70.7	904.4	1003.0	28.9	48.0	58.0	166.0	13.4	75.1
8	108.3	58.7	44.9	51.9	63.4	884.2	1001.0	70.8	904.4	1003.0	28.9	48.2	57.9	165.4	13.7	77.0
9	108.3	58.7	44.9	52.0	63.4	884.2	1001.1	70.8	904.3	1002.9	28.9	48.2	57.5	165.5	13.9	80.3
10	101.8	53.3	46.8	44.8	55.0	888.7	1002.8	68.0	907.7	1005.2	31.0	48.4	61.3	112.2	18.1	115.1
11	114.7	56.8	45.3	50.2	69.4	883.7	1001.7	75.8	905.2	1003.5	29.3	50.9	55.2	173.2	19.0	83.1
12	112.3	58.2	45.2	51.3	67.2	883.5	1001.3	73.7	904.6	1003.2	29.1	48.2	57.6	167.8	19.0	95.5
13	109.8	58.9	45.0	52.1	64.9	883.7	1001.0	71.8	904.3	1002.9	28.9	48.1	58.0	164.3	19.1	80.6
14	109.0	58.9	45.0	52.0	64.0	883.9	1001.0	71.2	904.3	1002.9	28.9	48.2	57.9	164.5	19.0	85.2
15	104.6	53.5	47.1	45.0	57.6	887.8	1002.7	69.9	907.5	1005.1	31.1	46.1	59.7	111.4	23.5	123.7
16	114.0	57.1	44.6	50.4	69.4	883.8	1001.6	75.2	905.3	1003.4	28.8	50.8	55.4	173.7	23.6	88.9
17	115.8	58.1	45.0	50.9	70.8	882.8	1001.3	76.1	904.9	1003.3	29.1	50.9	54.5	170.6	23.6	96.9
18	115.3	58.1	45.0	51.2	70.3	882.9	1001.3	75.8	904.7	1003.2	29.0	50.8	53.9	169.2	23.4	76.9
19	107.8	58.9	44.8	51.7	62.9	884.2	1001.0	70.3	904.5	1003.0	28.8	48.3	56.1	166.8	23.4	83.0
20	121.7	53.7	49.7	47.5	72.0	883.8	1002.8	81.8	905.4	1004.4	32.6	49.6	39.5	118.8	29.8	123.9
21	109.7	56.8	44.8	49.9	64.9	884.9	1001.7	72.3	905.5	1003.6	29.0	50.0	53.9	176.4	29.7	113.1
22	108.6	58.8	44.7	51.9	63.9	884.1	1001.0	71.0	904.4	1003.0	28.8	49.0	55.2	166.1	29.8	118.5
23	107.5	59.1	44.7	52.1	62.8	884.2	1000.9	70.1	904.3	1002.9	28.8	48.7	56.2	165.1	29.8	116.1
24	104.6	53.6	47.4	45.4	57.2	887.8	1002.7	69.8	907.2	1005.0	31.3	49.6	59.6	109.2	34.9	189.3
25	111.1	56.3	49.5	48.6	61.7	884.8	1001.9	73.5	904.9	1004.0	32.4	38.5	57.5	115.4	35.2	131.6
26	111.1	56.5	49.5	48.7	61.6	884.7	1001.8	73.4	904.8	1004.0	32.4	38.3	58.3	115.2	35.4	131.7
27	111.1	56.6	49.5	48.7	61.7	884.7	1001.8	73.4	904.9	1004.0	32.4	38.2	59.2	115.3	35.5	125.7
28	115.6	56.5	47.4	49.0	68.2	883.7	1001.8	76.5	905.3	1003.9	30.9	45.1	55.7	117.2	35.1	142.8
29	114.4	56.2	46.9	48.5	67.4	884.1	1001.9	75.8	905.6	1004.0	30.6	45.6	56.2	119.4	36.0	152.0
30	115.0	56.5	47.3	48.9	67.8	883.8	1001.9	76.2	905.4	1003.9	30.8	45.3	56.0	117.8	35.6	142.7
31	115.3	56.5	47.1	49.0	68.2	883.8	1001.9	76.3	905.4	1003.9	30.7	45.2	55.4	117.9	35.3	146.2
32	115.6	56.5	47.6	48.9	67.9	883.7	1001.8	76.5	905.3	1003.9	31.1	45.0	55.8	117.0	35.4	148.6
33	119.6	54.6	45.5	49.0	74.1	883.8	1002.5	80.0	905.8	1003.9	29.6	48.0	38.6	120.0	35.9	156.3
34	118.9	54.5	45.5	48.7	73.4	884.0	1002.5	79.6	905.9	1004.0	29.6	47.9	38.7	120.8	35.9	154.2
35	119.1	54.7	45.5	49.0	73.6	883.9	1002.5	79.6	905.8	1003.9	29.6	48.0	39.4	119.9	35.8	154.8
36	118.7	54.6	45.5	48.7	73.1	884.0	1002.5	79.3	906.0	1004.0	29.7	48.1	39.6	121.2	35.9	153.2
37	118.6	54.6	45.8	48.6	72.9	884.0	1002.5	79.3	905.9	1004.0	29.8	48.0	39.8	120.9	35.9	153.2
38	118.7	54.6	46.2	48.3	72.5	884.0	1002.5	79.4	906.0	1004.1	30.2	48.1	39.9	121.4	35.9	152.5
39	113.2	57.1	43.9	50.1	69.3	883.9	1001.6	74.7	905.6	1003.5	28.4	48.4	53.7	135.6	35.4	169.5
40	104.3	55.2	57.0	49.0	47.3	887.0	1002.2	69.1	902.5	1003.9	37.5	31.8	56.9	103.9	39.2	156.0

Flow period	Bulk density G	Bulk Density W	Bulk density O	den L mix	Liq den fraction	Density mix	S.G	Cv	Q/Cv	(Q/Cv)sq	Cv(m)	dP
1	41.9691	466.3625	475.1029	941.4654	372.4510672	414.4202	0.4144	16.8193	4.132742	17.07955	14.54195	7.08
2	41.5487	460.6584	480.2270	940.8853	376.8450516	418.3937	0.4184	15.8774	4.409217	19.44119	13.7276	8.13
3	41.7029	473.8625	468.4918	942.3543	377.4631272	419.1660	0.4192	22.8694	3.277899	10.74462	19.7729	4.50
4	45.1741	432.7248	503.7577	936.4826	319.206362	364.3805	0.3644	31.3385	1.816785	3.300709	27.09528	1.20
5	46.7329	432.2125	504.0520	936.2645	323.3154839	370.0484	0.3700	30.1799	2.332057	5.438489	26.09356	2.01
6	46.8550	431.2005	504.8555	936.0560	320.7619036	367.6169	0.3676	29.8340	1.601477	2.564728	25.79448	0.94
7	41.0155	480.3933	459.9159	940.3092	395.0277064	436.0432	0.4360	30.1209	2.885372	8.325371	26.04257	3.63
8	40.9518	482.7011	457.8251	940.5262	396.1827694	437.1345	0.4371	30.7176	2.898322	8.400272	26.55842	3.67
9	40.7281	482.6789	457.8602	940.5391	399.4245205	440.1526	0.4402	31.1075	2.984837	8.909253	26.89558	3.92
10	41.6492	485.2267	458.6496	943.8763	365.4686405	407.1178	0.4071	40.4932	3.286258	10.79949	35.01044	4.40
11	41.8493	509.4618	434.2828	943.7446	422.8508914	464.7002	0.4647	42.5175	2.261094	5.112546	36.76062	2.38
12	42.4647	482.3716	457.8857	940.2573	398.6190763	441.0838	0.4411	42.6094	2.591178	6.714203	36.84007	2.96
13	41.6356	481.3041	458.7930	940.0970	394.6987579	436.3343	0.4363	42.7847	2.177619	4.742026	36.99168	2.07
14	41.2151	482.1507	458.1671	940.3178	396.0222054	437.2373	0.4372	42.6998	2.306693	5.320834	36.91827	2.33
15	41.6975	462.6826	478.1668	940.8494	379.3988785	421.0964	0.4211	52.5469	2.723532	7.417625	45.43206	3.12
16	41.6512	509.2338	434.4612	943.6950	421.2841301	462.9354	0.4629	52.3172	1.964487	3.859211	45.23341	1.79
17	41.4705	509.6797	433.4510	943.1307	429.2485296	470.7191	0.4707	52.3943	2.139345	4.576795	45.30011	2.15
18	40.8453	508.7005	434.3576	943.0582	434.7670013	475.6123	0.4756	53.3707	1.667173	2.779467	46.14427	1.32
19	39.4666	483.6784	456.9437	940.6222	412.9269436	452.3935	0.4524	52.4958	1.829463	3.346934	45.38788	1.51
20	32.3275	496.9303	445.8283	942.7587	570.1549703	602.4824	0.6025	66.7376	2.14808	4.614247	57.7013	2.78
21	39.0110	500.7765	442.5113	943.2878	434.5553893	473.5664	0.4736	66.6072	1.9645	3.85926	57.58855	1.83
22	39.1586	490.8784	450.5453	941.4237	422.0802103	461.2388	0.4612	66.7724	2.051876	4.210193	57.7314	1.94
23	39.4240	487.0350	453.9454	940.9805	412.1021277	451.5261	0.4515	66.7290	2.012243	4.049124	57.6939	1.83
24	41.6512	497.7198	447.0981	944.8179	381.3200873	422.9713	0.4230	78.2069	2.799767	7.838698	67.61768	3.32
25	42.2819	385.8422	544.0532	929.8954	395.0209474	437.3028	0.4373	78.9228	1.928633	3.719625	68.23667	1.63
26	42.7887	383.7196	545.8486	929.5683	387.6763533	430.4650	0.4305	79.2515	1.921824	3.693409	68.52083	1.59
27	43.4436	382.4825	546.8984	929.3808	379.2361472	422.6797	0.4227	79.4163	1.831317	3.353724	68.66332	1.42
28	42.6313	451.5089	485.4353	936.9442	415.0108007	457.6421	0.4576	78.6168	2.101536	4.416455	67.97212	2.02
29	42.6116	456.9499	480.8955	937.8453	410.4190067	453.0306	0.4530	80.5998	2.181079	4.757104	69.68659	2.16
30	42.6882	453.6099	483.6654	937.2753	411.9550624	454.6433	0.4546	79.8152	2.068088	4.276989	69.00819	1.94
31	42.3256	452.8467	484.3089	937.1557	417.5482023	459.8738	0.4599	79.0412	2.138815	4.57453	68.33906	2.10
32	42.7312	451.1401	485.7627	936.9028	413.7713732	456.5025	0.4565	79.3771	2.164539	4.685229	68.62941	2.14
33	30.8545	481.0928	459.6484	940.7412	577.9099207	608.7644	0.6088	79.9288	2.262018	5.116723	69.10642	3.11
34	30.8114	479.8971	460.8374	940.7345	576.4242467	607.2356	0.6072	80.0170	2.228308	4.965357	69.18268	3.02
35	31.3560	481.2004	459.5989	940.7993	570.2289971	601.5850	0.6016	81.0408	2.209695	4.882751	70.06786	2.94
36	31.4094	481.9859	458.9622	940.9482	568.4582699	599.8676	0.5999	80.3263	2.205547	4.864438	69.45014	2.92
37	31.5497	481.3142	459.5829	940.8971	566.6796752	598.2294	0.5982	80.3876	2.204165	4.858345	69.50309	2.91
38	31.6905	482.2746	458.7270	941.0016	565.3560074	597.0465	0.5970	80.3922	2.194011	4.813685	69.50709	2.87
39	40.1196	484.7716	456.0937	940.8654	435.490606	475.6102	0.4756	79.4039	2.468612	6.094044	68.65258	2.90
40	39.3313	318.8013	604.8377	923.6391	398.0372787	437.3685	0.4374	87.7570	2.0564	4.228779	75.87474	1.85

Flow period	Oil avg.	Water Avg.	Gas Avg.	mass den g	mass den w	mass oil d	Liq mix	liq den fr	total mix	S.G	Cv	q/Cv	(q/Cv)sq	dP1
1	897.9	1004.0	50.3	30.3774726	466.911698	480.3178	947.2295	374.7314	405.1089	0.4051	16.8193	4.132742	17.07955	6.919078
2	898.0	1004.0	50.2	30.0899447	461.194828	485.4706	946.6654	379.1601	409.25	0.4093	15.8774	4.409217	19.44119	7.956308
3	897.9	1004.0	50.3	30.1746588	474.420053	473.6423	948.0623	379.7495	409.9242	0.4099	22.8694	3.277899	10.74462	4.404479
4	896.5	1003.2	50.0	32.985017	433.294763	509.3119	942.6067	321.2938	354.2788	0.3543	31.3385	1.816785	3.300709	1.169371
5	896.5	1003.5	51.5	33.7402098	432.779475	509.8808	942.6602	325.5241	359.2643	0.3593	30.1799	2.332057	5.438489	1.953855
6	896.4	1003.5	51.5	33.8408402	431.773859	510.7054	942.4792	322.963	356.8038	0.3568	29.8340	1.601477	2.564728	0.915105
7	894.3	1002.0	49.8	28.8923784	480.849672	465.1495	945.9992	397.4181	426.3105	0.4263	30.1209	2.885372	8.325371	3.549193
8	894.3	1002.0	49.8	28.828614	483.164699	463.0548	946.2195	398.581	427.4096	0.4274	30.7176	2.898322	8.400272	3.590357
9	894.3	1002.0	49.8	28.6656401	483.134195	463.0771	946.2113	401.8334	430.499	0.4305	31.1075	2.984837	8.909253	3.835424
10	898.2	1004.0	49.5	30.3083494	485.800078	463.5624	949.3624	367.5929	397.9012	0.3979	40.4932	3.286258	10.79949	4.29713
11	894.5	1002.6	52.6	29.0189956	509.911501	439.5538	949.4653	425.4141	454.4331	0.4544	42.5175	2.261094	5.112546	2.32331
12	894.1	1002.2	51.4	29.6256396	482.826731	463.3444	946.1711	401.1262	430.7519	0.4308	42.6094	2.591178	6.714203	2.892156
13	894.0	1001.9	50.3	29.2050747	481.76632	464.128	945.8943	397.1327	426.3378	0.4263	42.7847	2.177619	4.742026	2.021705
14	894.1	1002.0	50.1	28.9737121	482.6162	463.4456	946.0618	398.4413	427.4151	0.4274	42.6998	2.306693	5.320834	2.274205
15	897.7	1003.9	50.5	30.1405372	463.232382	483.4648	946.6972	381.757	411.8975	0.4119	52.5469	2.723532	7.417625	3.055301
16	894.5	1002.5	52.0	28.8051941	509.690885	439.7526	949.4434	423.8504	452.6555	0.4527	52.3172	1.964487	3.859211	1.746893
17	893.9	1002.3	52.6	28.6506888	510.182332	438.8797	949.062	431.9481	460.5988	0.4606	52.3943	2.139345	4.576795	2.108066
18	893.8	1002.3	52.4	28.2513034	509.180731	439.7304	948.9111	437.4653	465.7166	0.4657	53.3707	1.667173	2.779467	1.294444
19	894.4	1002.0	49.6	27.815812	484.17577	462.1966	946.3724	415.4512	443.2671	0.4433	52.4958	1.829463	3.346934	1.483585
20	894.6	1003.6	57.2	22.6147459	497.322387	451.2851	948.6075	573.6922	596.3069	0.5963	66.7376	2.14808	4.614247	2.751508
21	895.2	1002.7	50.7	27.328247	501.256176	447.6695	948.9257	437.1527	464.4809	0.4645	66.6072	1.9645	3.85926	1.792553
22	894.3	1002.0	49.9	27.5127214	491.356489	455.7376	947.0941	424.6225	452.1352	0.4521	66.7724	2.051876	4.210193	1.903577
23	894.3	1001.9	49.4	27.7914964	487.520121	459.1224	946.6425	414.5818	442.3733	0.4424	66.7290	2.012243	4.049124	1.791224
24	897.5	1003.8	50.6	30.1709694	498.287624	451.9806	950.2682	383.5198	413.6908	0.4137	78.2069	2.799767	7.838698	3.242797
25	894.8	1002.9	52.9	30.4488122	386.255352	550.2175	936.4729	397.8151	428.2639	0.4283	78.9228	1.928633	3.719625	1.592981
26	894.8	1002.9	52.9	30.8300336	384.141388	552.0562	936.1976	390.4411	421.2711	0.4213	79.2515	1.921824	3.693409	1.555926
27	894.8	1002.9	52.9	31.2996698	382.908258	553.1363	936.0445	381.9553	413.255	0.4133	79.4163	1.831317	3.353724	1.385943
28	894.5	1002.9	53.7	29.9162967	451.972541	491.3625	943.3351	417.8415	447.7578	0.4478	78.6168	2.101536	4.416455	1.977503
29	894.9	1003.0	53.2	29.9189582	457.432206	486.7477	944.1799	413.1912	443.1101	0.4431	80.5998	2.181079	4.757104	2.107921
30	894.6	1002.9	53.5	29.9801733	454.081569	489.5553	943.6369	414.7511	444.7313	0.4447	79.8152	2.068088	4.276989	1.902111
31	894.6	1002.9	53.5	29.6629755	453.30883	490.2214	943.5302	420.3884	450.0514	0.4501	79.0412	2.138815	4.57453	2.058773
32	894.5	1002.9	53.8	30.0385704	451.610965	491.6902	943.3011	416.5971	446.6357	0.4466	79.3771	2.164539	4.685229	2.09259
33	894.8	1003.2	54.8	21.1363565	481.432526	465.3746	946.8071	581.6363	602.7727	0.6028	79.9288	2.262018	5.116723	3.084221
34	895.0	1003.2	54.6	21.1448843	480.246649	466.554	946.8007	580.1412	601.2861	0.6013	80.0170	2.228308	4.965357	2.9856
35	894.8	1003.2	54.6	21.5115606	481.547236	465.3019	946.8491	573.8959	595.4074	0.5954	81.0408	2.209695	4.882751	2.907227
36	895.0	1003.2	54.5	21.5764689	482.354027	464.6705	947.0245	572.1292	593.7057	0.5937	80.3263	2.205547	4.864438	2.888044
37	895.0	1003.3	54.6	21.7044831	481.683185	465.2824	946.9656	570.3346	592.039	0.5920	80.3876	2.204165	4.858345	2.87633
38	895.0	1003.3	54.8	21.8648296	482.664528	464.426	947.0905	569.0143	590.8791	0.5909	80.3922	2.194011	4.813685	2.844306
39	894.8	1002.6	51.5	27.6877199	485.234714	461.7014	946.9362	438.3005	465.9883	0.4660	79.4039	2.468612	6.094044	2.839753
40	894.8	1003.0	53.3	30.3346599	319.076246	610.1312	929.2074	400.4369	430.7716	0.4308	87.7570	2.0564	4.228779	1.821638

Flow period	Pressure [bar]	Temp. [C]	Pressure [bar]	Temperature [C]	dP [bar]	Oil	Water	Gas	Oil	Water	Gas	WLR	GVF	Viscosity [cP]	Choke position [%]	Total flow [Am3/h]
41	111.9	56.4	48.5	49.4	63.5	884.6	1001.8	74.0	904.7	1003.8	31.6	37.8	51.5	114.2	40.3	179.7
42	113.2	56.7	48.5	49.3	64.8	884.1	1001.8	74.8	904.8	1003.8	31.6	38.2	53.8	114.3	39.0	169.7
43	111.8	56.0	46.0	48.9	65.8	884.8	1002.0	74.1	905.7	1003.9	30.0	46.8	54.9	119.6	40.0	190.7
44	113.9	56.0	46.0	48.7	68.0	884.3	1002.0	75.6	905.8	1004.0	30.0	46.2	52.9	120.3	41.0	202.0
45	112.2	56.1	46.0	48.8	66.3	884.7	1002.0	74.4	905.7	1003.9	29.9	46.0	53.2	119.8	40.9	199.0
46	113.1	55.9	46.0	48.7	67.2	884.6	1002.0	75.0	905.8	1004.0	29.9	46.3	53.0	120.4	40.4	193.2
47	120.5	54.0	45.5	48.7	75.1	883.9	1002.7	80.9	906.0	1004.0	29.6	49.0	34.5	121.1	39.5	178.5
48	120.5	54.2	45.5	48.8	75.0	883.8	1002.6	80.8	905.9	1003.9	29.6	49.2	35.2	120.4	39.5	179.2
49	120.3	54.0	45.5	48.5	74.7	884.0	1002.7	80.7	906.1	1004.0	29.7	49.1	35.2	121.7	39.5	181.6
50	120.6	54.1	45.5	48.7	75.1	883.8	1002.6	80.9	905.9	1004.0	29.6	49.2	35.7	121.1	39.5	182.5
51	106.0	57.2	53.5	51.3	52.5	885.6	1001.6	69.7	902.3	1003.2	34.8	48.2	53.9	151.7	40.9	183.9
52	105.9	57.1	53.5	50.8	52.4	885.6	1001.6	69.7	902.5	1003.3	34.8	48.1	53.8	153.8	40.9	184.7
53	105.0	53.8	48.9	45.9	56.0	887.6	1002.7	70.0	906.5	1004.8	32.3	49.2	59.4	105.6	46.3	281.8
54	95.7	55.0	48.2	47.3	47.5	889.2	1002.2	63.2	906.0	1004.4	31.7	41.7	62.6	130.6	45.7	243.8
55	95.7	54.8	48.3	47.1	47.4	889.3	1002.3	63.2	906.1	1004.5	31.7	41.7	62.4	131.4	45.7	237.7
56	95.9	54.8	48.3	47.1	47.6	889.3	1002.3	63.4	906.0	1004.5	31.8	41.9	61.9	131.1	45.7	231.9
57	96.2	54.9	48.2	47.1	48.0	889.2	1002.2	63.6	906.0	1004.5	31.7	42.0	62.2	131.0	45.7	237.8
58	96.7	55.7	48.2	47.3	48.4	888.6	1002.0	63.7	906.0	1004.4	31.7	41.1	65.7	130.8	45.7	224.8
59	97.6	55.9	48.3	47.1	49.3	888.3	1001.9	64.2	906.0	1004.5	31.7	41.4	66.9	131.3	45.7	213.3
60	99.4	56.2	48.4	47.3	51.0	887.6	1001.8	65.4	905.9	1004.4	31.8	41.9	67.2	130.3	45.7	196.0
61	99.2	56.4	48.3	47.4	51.0	887.6	1001.8	65.3	905.9	1004.4	31.7	41.7	67.0	129.9	45.7	200.3
62	98.9	56.2	48.3	47.4	50.7	887.8	1001.8	65.1	905.9	1004.4	31.7	41.7	66.7	130.3	45.7	203.6
63	110.7	57.5	45.8	50.3	64.9	884.3	1001.5	72.8	905.0	1003.5	29.7	45.6	53.3	131.7	45.9	301.8
64	108.7	57.3	45.8	50.1	62.8	884.9	1001.5	71.5	905.1	1003.5	29.7	45.8	53.4	132.6	45.3	293.0
65	108.8	57.6	45.3	50.4	63.5	884.7	1001.4	71.5	905.1	1003.5	29.3	45.7	53.8	132.5	45.5	293.8
66	100.4	56.1	49.1	48.1	51.3	887.5	1001.9	66.1	905.3	1004.2	32.1	42.0	61.8	126.1	50.3	334.1
67	102.3	56.9	48.2	48.5	54.2	886.6	1001.6	67.3	905.3	1004.1	31.5	40.7	62.2	125.9	50.7	310.5
68	98.3	55.8	48.2	47.9	50.1	888.1	1001.9	64.8	905.6	1004.2	31.6	41.0	62.6	128.3	50.7	316.8
69	96.4	55.5	48.3	47.7	48.2	888.7	1002.0	63.6	905.7	1004.3	31.7	41.0	62.8	128.8	50.7	305.7
70	96.3	55.6	48.3	47.7	48.0	888.8	1002.0	63.5	905.7	1004.3	31.7	41.2	63.4	128.9	50.7	303.6
71	96.5	55.6	48.3	47.7	48.3	888.7	1002.0	63.6	905.7	1004.3	31.7	41.7	63.1	128.7	50.7	307.5
72	95.8	55.5	48.3	47.7	47.5	888.9	1002.0	63.1	905.7	1004.3	31.7	41.4	63.1	128.8	50.7	305.4
73	96.1	55.4	48.3	47.6	47.8	888.9	1002.1	63.4	905.8	1004.3	31.7	41.4	62.8	129.2	50.7	299.6
74	95.8	55.3	48.3	47.6	47.5	889.0	1002.1	63.2	905.8	1004.3	31.7	41.7	62.7	129.3	50.3	295.1
75	108.5	56.1	47.5	50.9	61.0	885.6	1001.9	71.7	904.2	1003.3	30.8	36.9	42.8	110.6	50.5	284.1
76	109.1	50.2	43.3	45.8	65.7	888.5	1003.8	74.2	908.1	1004.9	28.5	57.7	37.5	136.2	50.2	297.8
77	113.9	51.9	38.5	46.7	75.4	886.5	1003.3	77.0	909.1	1004.6	25.1	57.7	42.9	141.8	50.7	300.2
78	106.2	58.9	48.7	53.8	57.5	884.6	1001.0	69.3	902.3	1002.4	31.2	50.3	52.1	149.8	55.2	358.1
79	106.1	59.1	48.8	54.1	57.3	884.5	1000.9	69.2	902.1	1002.3	31.2	50.4	52.1	148.0	55.2	354.7
80	95.6	57.1	43.8	54.0	51.8	888.1	1001.5	62.6	903.6	1002.3	27.9	51.6	41.0	158.0	55.6	336.7

Flow period	Bulk density G	Bulk Density W	Bulk density O	den L mix	Liq den fraction	Density mix	S.G	Cv	Q/Cv	(Q/Cv)sq	Cv(m)	dP
41	38.1494	378.5696	550.3336	928.9033	450.1213193	488.2707	0.4883	90.2353	2.303101	5.304275	78.01743	2.59
42	40.2269	382.9897	546.1036	929.0934	429.6355805	469.8625	0.4699	87.4184	2.245862	5.043897	75.58198	2.37
43	40.6529	469.2450	470.4366	939.6816	423.916396	464.5693	0.4646	89.5969	2.462313	6.062985	77.46547	2.82
44	40.0107	463.0117	475.6968	938.7086	441.6646764	481.6754	0.4817	91.7878	2.54556	6.479875	79.35975	3.12
45	39.5225	460.9627	477.6880	938.6507	439.7407839	479.2633	0.4793	91.5265	2.51415	6.320952	79.13384	3.03
46	39.7424	463.9186	475.0269	938.9455	441.5326651	481.2751	0.4813	90.4235	2.470959	6.105638	78.1802	2.94
47	27.9139	491.3905	450.7175	942.1079	616.9486948	644.8626	0.6449	88.6536	2.32918	5.42508	76.64993	3.50
48	28.4382	493.3820	448.8961	942.2781	610.5228055	638.9610	0.6390	88.6094	2.338573	5.468925	76.61165	3.49
49	28.4411	492.2974	449.9472	942.2446	610.1270289	638.5681	0.6386	88.5390	2.371721	5.625058	76.55082	3.59
50	28.8722	493.0168	449.2333	942.2502	605.7720853	634.6443	0.6346	88.0933	2.396465	5.743044	76.16548	3.64
51	37.5592	482.2796	459.1471	941.4267	433.9159019	471.4751	0.4715	91.4357	2.325718	5.408965	79.05529	2.55
52	37.4759	482.1715	459.2803	941.4518	435.1648297	472.6407	0.4726	92.3851	2.312863	5.349333	79.87618	2.53
53	41.6002	493.0120	451.1777	944.1897	383.4454803	425.0457	0.4250	103.6979	3.143148	9.879378	89.65717	4.20
54	39.5927	417.8292	518.4654	936.2946	349.776366	389.3690	0.3894	102.4202	2.753614	7.582391	88.55252	2.95
55	39.4596	417.8411	518.5647	936.4058	352.1567304	391.6164	0.3916	102.4044	2.684233	7.205109	88.53884	2.82
56	39.2585	419.5614	517.0264	936.5878	356.7310732	395.9896	0.3960	102.3880	2.61998	6.864297	88.52466	2.72
57	39.5836	420.8471	515.7989	936.6460	353.7618191	393.3454	0.3933	102.3917	2.68564	7.212663	88.52783	2.84
58	41.8201	411.9714	523.2499	935.2214	321.1001445	362.9202	0.3629	102.3624	2.539875	6.450967	88.5025	2.34
59	42.9728	415.1830	520.1679	935.3509	309.6818447	352.6547	0.3527	102.3493	2.41017	5.808917	88.49124	2.05
60	43.9441	419.8682	515.6213	935.4895	307.03487	350.9789	0.3510	102.3712	2.214144	4.902434	88.51013	1.72
61	43.7172	417.6991	517.5056	935.2046	308.7994174	352.5167	0.3525	102.3584	2.263687	5.12428	88.4991	1.81
62	43.4258	417.5285	517.7910	935.3195	311.450038	354.8758	0.3549	102.3780	2.299711	5.288672	88.51602	1.88
63	38.8163	456.7556	480.9798	937.7355	437.703089	476.5194	0.4765	102.7854	3.396355	11.53522	88.86821	5.50
64	38.1614	458.6919	479.5975	938.2893	437.5359112	475.6973	0.4757	101.5634	3.336927	11.13508	87.81174	5.30
65	38.4499	458.1592	479.9491	938.1084	433.6127768	472.0627	0.4721	102.0139	3.33141	11.09829	88.20119	5.24
66	40.8777	420.4749	515.0217	935.4966	357.1718287	398.0496	0.3980	112.6766	3.429289	11.76002	97.42022	4.68
67	41.8377	407.6711	525.7473	933.4183	352.8562584	394.6940	0.3947	113.3063	3.169121	10.04333	97.96464	3.96
68	40.5167	411.0889	523.7308	934.8197	350.0437908	390.5605	0.3906	113.4232	3.230659	10.43716	98.06568	4.08
69	39.9207	411.1117	524.1050	935.2167	347.8692848	387.7900	0.3878	113.6261	3.111865	9.683706	98.24114	3.76
70	40.2523	412.7173	522.6867	935.4040	342.0075237	382.2598	0.3823	113.6541	3.089773	9.546695	98.26533	3.65
71	40.1372	418.1018	517.8713	935.9731	345.4903552	385.6276	0.3856	113.6700	3.128396	9.786861	98.27905	3.77
72	39.7987	415.2218	520.5729	935.7947	345.7662539	385.5650	0.3856	113.6608	3.107935	9.659262	98.27116	3.72
73	39.7797	414.4817	521.2358	935.7175	348.3147313	388.0944	0.3881	113.6136	3.050387	9.304863	98.23033	3.61
74	39.6198	417.9874	518.1826	936.1700	348.9983582	388.6182	0.3886	112.6441	3.030256	9.182454	97.39205	3.57
75	30.7276	369.5982	558.8839	928.4822	530.8315675	561.5592	0.5616	113.2282	2.902422	8.424051	97.89707	4.73
76	27.8010	579.4866	375.5756	955.0623	597.1505145	624.9515	0.6250	112.4958	3.061723	9.374151	97.26383	5.86
77	32.9855	579.1759	374.7392	953.9151	545.1553672	578.1409	0.5781	113.4944	3.058986	9.357397	98.12725	5.41
78	36.1515	503.9714	439.2049	943.1763	451.405685	487.5572	0.4876	123.6075	3.350373	11.225	106.8711	5.47
79	36.0791	504.5474	438.6195	943.1669	451.3254533	487.4045	0.4874	123.6798	3.317344	11.00477	106.9336	5.36
80	25.6459	516.6381	429.9634	946.6015	558.642297	584.2882	0.5843	124.5338	3.127339	9.780247	107.6719	5.71

Flow period	Oil avg.	Water Avg.	Gas Avg.	mass den g	mass den w	mass oil d	Liq mix	liq den fr	total mix	S.G	Cv	q/Cv	(q/Cv)sq	dP1
41	894.7	1002.8	52.8	27.2132893	378.934541	556.6019	935.5364	453.3356	480.5489	0.4805	90.2353	2.303101	5.304275	2.548963
42	894.4	1002.8	53.2	28.6060141	383.379446	552.481	935.8604	432.7648	461.3709	0.4614	87.4184	2.245862	5.043897	2.327107
43	895.3	1003.0	52.0	28.5562363	469.706296	475.9931	945.6994	426.6312	455.1874	0.4552	89.5969	2.462313	6.062985	2.759794
44	895.1	1003.0	52.8	27.9375623	463.468716	481.4678	944.9365	444.5949	472.5325	0.4725	91.7878	2.54556	6.479875	3.061952
45	895.2	1003.0	52.2	27.7199477	461.417176	483.3668	944.7839	442.6141	470.334	0.4703	91.5265	2.51415	6.320952	2.972959
46	895.2	1003.0	52.5	27.801863	464.373863	480.7326	945.1064	444.4298	472.2317	0.4722	90.4235	2.470959	6.105638	2.883276
47	894.9	1003.3	55.3	19.0725703	491.710814	456.3428	948.0536	620.8423	639.9149	0.6399	88.6536	2.32918	5.42508	3.47159
48	894.9	1003.3	55.2	19.4340476	493.707643	454.5027	948.2103	614.3664	633.8005	0.6338	88.6094	2.338573	5.468925	3.466208
49	895.0	1003.4	55.2	19.4478596	492.634434	455.5764	948.2108	613.9903	633.4382	0.6334	88.5390	2.371721	5.625058	3.563127
50	894.9	1003.3	55.2	19.7264113	493.344804	454.8545	948.1993	609.5968	629.3232	0.6293	88.0933	2.396465	5.743044	3.614231
51	893.9	1002.4	52.2	28.1528176	482.67062	463.4742	946.1449	436.0906	464.2434	0.4642	91.4357	2.325718	5.408965	2.511076
52	894.1	1002.5	52.3	28.1034359	482.592517	463.6645	946.257	437.3859	465.4894	0.4655	92.3851	2.312863	5.349333	2.490058
53	897.1	1003.7	51.2	30.4047962	493.551357	455.972	949.5233	385.6115	416.0163	0.4160	103.6979	3.143148	9.879378	4.109983
54	897.6	1003.3	47.4	29.7162478	418.29818	523.3563	941.6545	351.7787	381.4949	0.3815	102.4202	2.753614	7.582391	2.892644
55	897.7	1003.4	47.5	29.6259381	418.305808	523.4417	941.7475	354.1656	383.7915	0.3838	102.4044	2.684233	7.205109	2.76526
56	897.7	1003.4	47.6	29.4603537	420.022534	521.8878	941.9103	358.7583	388.2187	0.3882	102.3880	2.61998	6.864297	2.664848
57	897.6	1003.4	47.6	29.6513328	421.312864	520.688	942.0009	355.7843	385.4356	0.3854	102.3917	2.68564	7.212663	2.780017
58	897.3	1003.2	47.7	31.3115392	412.475044	528.3566	940.8317	323.0264	354.3379	0.3543	102.3624	2.539875	6.450967	2.285822
59	897.1	1003.2	48.0	32.0983086	415.715594	525.3702	941.0858	311.5806	343.6789	0.3437	102.3493	2.41017	5.808917	1.996402
60	896.8	1003.1	48.6	32.6597384	420.416984	520.9243	941.3413	308.9555	341.6152	0.3416	102.3712	2.214144	4.902434	1.674746
61	896.7	1003.1	48.5	32.4713918	418.246868	522.8336	941.0805	310.7396	343.211	0.3432	102.3584	2.263687	5.12428	1.758709
62	896.8	1003.1	48.4	32.2856538	418.063396	523.0669	941.1303	313.385	345.6706	0.3457	102.3780	2.299711	5.288672	1.828138
63	894.6	1002.5	51.2	27.3171129	457.214009	486.6127	943.8267	440.5463	467.8634	0.4679	102.7854	3.396355	11.53522	5.396909
64	895.0	1002.5	50.6	26.9996632	459.154557	485.0868	944.2413	440.3114	467.3111	0.4673	101.5634	3.336927	11.13508	5.203548
65	894.9	1002.5	50.4	27.1134135	458.62104	485.4833	944.1043	436.3842	463.4977	0.4635	102.0139	3.33141	11.09829	5.144033
66	896.4	1003.0	49.1	30.3741086	420.960246	520.1832	941.1434	359.3278	389.7019	0.3897	112.6766	3.429289	11.76002	4.582903
67	896.0	1002.8	49.4	30.7086349	408.164827	531.2956	939.4605	355.1403	385.849	0.3858	113.3063	3.169121	10.04333	3.875207
68	896.9	1003.1	48.2	30.1418748	411.562974	528.8938	940.4568	352.1546	382.2965	0.3823	113.4232	3.230659	10.43716	3.990089
69	897.2	1003.2	47.6	29.9000774	411.579908	529.1127	940.6926	349.9061	379.8062	0.3798	113.6261	3.111865	9.683706	3.677932
70	897.2	1003.2	47.6	30.1681687	413.190868	527.6778	940.8687	344.0055	374.1737	0.3742	113.6541	3.089773	9.546695	3.572122
71	897.2	1003.2	47.6	30.0549759	418.580338	522.8318	941.4122	347.4981	377.553	0.3776	113.6700	3.128396	9.786861	3.695059
72	897.3	1003.2	47.4	29.8870679	415.69346	525.4909	941.1844	347.7577	377.6448	0.3776	113.6608	3.107935	9.659262	3.64777
73	897.3	1003.2	47.5	29.8335239	414.950136	526.1805	941.1306	350.3297	380.1632	0.3802	113.6136	3.050387	9.304863	3.537367
74	897.4	1003.2	47.4	29.7448887	418.456705	523.0678	941.5245	350.9945	380.7394	0.3807	112.6441	3.030256	9.182454	3.496122
75	894.9	1002.6	51.3	21.9510195	369.853784	564.7674	934.6212	534.3414	556.2924	0.5563	113.2282	2.902422	8.424051	4.686235
76	898.3	1004.3	51.3	19.2370145	579.799241	379.7206	959.5199	599.9376	619.1746	0.6192	112.4958	3.061723	9.374151	5.804236
77	897.8	1003.9	51.0	21.8632699	579.555031	379.5105	959.0655	548.0988	569.9621	0.5700	113.4944	3.058986	9.357397	5.333361
78	893.4	1001.7	50.3	26.2147919	504.322701	443.6014	947.9241	453.678	479.8928	0.4799	123.6075	3.350373	11.225	5.386796
79	893.3	1001.6	50.2	26.1830894	504.888587	442.9789	947.8674	453.5748	479.7579	0.4798	123.6798	3.317344	11.00477	5.279627
80	895.8	1001.9	45.3	18.5457335	516.840895	433.7041	950.545	560.9696	579.5153	0.5795	124.5338	3.127339	9.780247	5.667803

Flow period	Pressure [bar]	Temp. [C]	Pressure [bar]	Temperature [C]	dP [bar]	Oil	Water	Gas	Oil	Water	Gas	WLR	GVF	Viscosity [cP]	Choke position [%]	Total flow [Am3/h]
81	99.9	57.4	46.4	53.6	53.5	886.9	1001.4	65.4	903.0	1002.4	29.7	51.6	42.6	154.8	55.6	356.9
82	101.4	58.5	43.4	54.1	58.0	885.9	1001.1	66.1	903.6	1002.2	27.6	51.4	47.9	158.1	55.6	395.0
83	104.0	59.3	47.7	54.2	56.3	884.9	1000.8	67.7	902.3	1002.2	30.5	49.1	53.8	149.6	55.2	344.0
84	104.0	59.4	47.1	54.2	56.9	884.8	1000.8	67.7	902.5	1002.2	30.1	49.2	54.2	150.8	55.2	346.9
85	105.7	58.5	49.1	53.6	56.6	884.9	1001.1	69.1	902.3	1002.4	31.5	49.9	51.6	150.0	55.2	329.1
86	111.7	50.2	48.3	45.4	63.4	887.9	1003.8	76.0	907.0	1005.0	32.0	57.1	44.1	128.8	54.8	330.0
87	109.5	48.2	60.6	44.9	48.9	889.4	1004.4	75.2	903.8	1005.2	40.7	56.2	30.8	112.0	55.1	317.8
88	109.5	48.1	60.5	44.6	48.9	889.5	1004.4	75.2	904.0	1005.2	40.7	56.7	30.4	112.8	55.3	317.5
89	106.0	58.0	49.1	53.1	56.8	885.1	1001.3	69.4	902.5	1002.6	31.6	49.0	51.8	151.8	55.2	350.9
90	95.6	57.1	43.8	54.0	51.8	888.1	1001.5	62.6	903.6	1002.3	27.9	51.6	41.0	158.0	55.6	336.7
91	106.2	57.7	49.0	52.9	57.2	885.2	1001.4	69.7	902.7	1002.7	31.5	49.0	51.8	153.3	55.2	353.5
92	99.9	57.4	46.4	53.6	53.5	886.9	1001.4	65.4	903.0	1002.4	29.7	51.6	42.6	154.8	55.6	356.9
93	106.1	57.9	49.1	53.1	57.0	885.1	1001.3	69.6	902.5	1002.6	31.6	48.8	51.9	152.1	55.2	352.2
94	101.4	58.5	43.4	54.1	58.0	885.9	1001.1	66.1	903.6	1002.2	27.6	51.4	47.9	158.1	55.6	395.0
95	114.2	54.3	48.8	50.2	65.4	885.2	1002.6	76.4	904.2	1003.5	31.7	44.3	32.0	111.0	55.6	341.0
96	114.4	50.7	47.6	46.0	66.8	887.0	1003.6	77.7	906.8	1004.8	31.4	61.0	43.9	127.9	55.9	370.9
97	103.8	48.7	53.9	44.6	49.8	890.6	1004.2	70.9	905.8	1005.2	36.0	55.0	41.1	122.7	55.3	333.9
98	105.4	49.7	51.9	45.3	53.5	889.7	1003.9	71.7	906.0	1005.0	34.5	55.0	42.3	123.0	56.1	353.4
99	99.4	47.2	47.5	44.3	51.8	892.4	1004.6	68.2	907.8	1005.3	31.6	62.2	24.5	134.5	55.7	342.8
100	111.9	50.2	48.6	45.4	63.3	887.9	1003.8	76.2	906.9	1005.0	32.2	57.3	43.8	128.2	55.3	339.9
101	111.7	50.2	48.3	45.4	63.4	887.9	1003.8	76.0	907.0	1005.0	32.0	57.1	44.1	128.8	54.8	330.0
102	109.5	48.2	60.6	44.9	48.9	889.4	1004.4	75.2	903.8	1005.2	40.7	56.2	30.8	112.0	55.1	317.8
103	106.8	58.5	49.5	51.2	57.3	884.7	1001.1	69.9	903.5	1003.2	32.1	47.3	56.6	114.6	59.2	530.9
104	102.1	57.6	49.6	50.4	52.6	886.3	1001.4	66.9	903.9	1003.5	32.2	45.1	57.4	117.3	59.2	529.6
105	98.9	55.8	49.6	48.9	49.3	888.0	1001.9	65.2	904.7	1003.9	32.4	44.9	57.7	122.2	59.2	536.6
106	98.3	55.8	49.6	48.9	48.7	888.2	1002.0	64.8	904.7	1003.9	32.4	44.9	57.5	122.3	59.2	535.5
107	97.6	55.8	49.5	49.0	48.1	888.3	1002.0	64.3	904.7	1003.9	32.3	41.9	57.1	122.0	59.1	509.3
108	98.0	56.2	49.5	49.3	48.5	888.0	1001.8	64.5	904.5	1003.8	32.3	44.2	58.5	121.0	59.1	545.8
109	98.6	56.4	49.6	49.6	49.0	887.7	1001.7	64.8	904.3	1003.7	32.3	43.6	58.5	120.1	59.2	542.7
110	100.0	56.8	49.5	49.5	50.4	887.2	1001.6	65.7	904.4	1003.7	32.3	42.7	60.1	120.3	58.2	522.6
111	89.6	51.0	49.7	47.7	39.9	892.9	1003.4	60.0	905.3	1004.3	32.6	43.1	29.4	118.2	59.2	375.3
112	113.5	49.7	45.5	45.8	68.0	887.8	1003.9	77.5	907.5	1004.9	30.0	60.0	30.2	132.0	59.0	398.2
113	110.8	49.1	47.9	45.8	62.9	888.7	1004.1	75.7	906.8	1004.9	31.6	62.5	25.1	127.9	59.7	464.3
114	110.6	49.4	46.5	45.7	64.1	888.6	1004.0	75.6	907.3	1004.9	30.7	59.6	28.3	130.6	58.9	399.8
115	78.4	42.5	51.9	38.6	26.6	900.1	1005.8	54.1	909.5	1006.9	35.4	64.3	20.1	160.8	65.3	420.7
116	93.0	42.2	52.0	41.4	40.9	896.6	1006.0	65.0	908.0	1006.1	35.1	65.3	17.1	137.8	62.9	405.5
117	72.0	43.3	50.5	42.9	21.5	901.4	1005.6	49.2	907.6	1005.7	33.8	63.3	19.9	154.9	70.5	445.5
118	87.8	52.6	46.1	50.4	41.7	892.5	1002.9	58.3	904.8	1003.4	29.9	56.2	23.3	170.8	64.3	473.7

Flow period	Bulk density G	Bulk Density W	Bulk density O	den L mix	Liq den fraction	Density mix	S.G	Cv	Q/Cv	(Q/Cv)sq	Cv(m)	dP
81	27.8938	516.3939	429.5538	945.9478	542.646918	570.5407	0.5705	124.5482	3.314491	10.98585	107.6844	6.27
82	31.6535	514.3547	430.7175	945.0723	492.6350653	524.2886	0.5243	124.5407	3.668194	13.45565	107.6779	7.05
83	36.4181	491.7712	450.0581	941.8293	435.0039308	471.4221	0.4714	123.4094	3.223888	10.39345	106.6998	4.90
84	36.6427	492.4424	449.4427	941.8851	431.809193	468.4519	0.4685	123.4981	3.248817	10.55481	106.7764	4.94
85	35.6910	499.3270	443.5494	942.8764	455.9356575	491.6266	0.4916	123.7327	3.076545	9.46513	106.9793	4.65
86	33.5577	573.3148	380.7731	954.0879	532.8784299	566.4361	0.5664	122.8364	3.107049	9.653751	106.2044	5.47
87	23.1243	564.3193	389.6834	954.0027	660.5871619	683.7115	0.6837	123.5004	2.976707	8.860784	106.7785	6.06
88	22.8361	569.0072	385.6015	954.6087	664.6461798	687.4822	0.6875	123.7682	2.966716	8.801403	107.01	6.05
89	35.9853	490.8570	451.2191	942.0761	453.7004094	489.6857	0.4897	123.7058	3.280337	10.76061	106.956	5.27
90	25.6459	516.6381	429.9634	946.6015	558.642297	584.2882	0.5843	124.4912	3.128408	9.786935	107.6351	5.72
91	36.0945	490.5832	451.5475	942.1307	453.9947833	490.0893	0.4901	123.6937	3.30573	10.92785	106.9456	5.36
92	27.8938	516.3939	429.5538	945.9478	542.646918	570.5407	0.5705	124.5228	3.315167	10.99033	107.6624	6.27
93	36.0999	488.7992	453.0316	941.8308	453.0036154	489.1036	0.4891	123.7001	3.293401	10.84649	106.9511	5.31
94	31.6535	514.3547	430.7175	945.0723	492.6350653	524.2886	0.5243	124.5508	3.667897	13.45347	107.6866	7.05
95	24.4345	443.8905	493.2766	937.1670	637.2602784	661.6948	0.6617	124.5149	3.167436	10.03265	107.6556	6.64
96	34.1248	612.3693	345.8110	958.1803	537.562176	571.6869	0.5717	125.2958	3.42416	11.72487	108.3308	6.70
97	29.1369	552.5948	400.4969	953.0917	561.1982844	590.3352	0.5903	123.9800	3.115369	9.705525	107.1931	5.73
98	30.3158	552.0909	400.3972	952.4881	549.6183845	579.9342	0.5799	125.6251	3.25337	10.58442	108.6155	6.14
99	16.6859	624.5598	337.5953	962.1550	726.583628	743.2695	0.7433	124.6999	3.179922	10.11191	107.8155	7.52
100	33.3617	575.3431	378.9764	954.3195	536.3233572	569.6851	0.5697	123.9384	3.171522	10.05855	107.1571	5.73
101	33.5577	573.3148	380.7731	954.0879	532.8784299	566.4361	0.5664	122.5299	3.114822	9.702115	105.9393	5.50
102	23.1243	564.3193	389.6834	954.0027	660.5871619	683.7115	0.6837	123.2934	2.981704	8.89056	106.5995	6.08
103	39.5333	473.9632	465.8365	939.7997	408.0768207	447.6101	0.4476	132.5818	4.631506	21.45085	114.6302	9.60
104	38.4134	451.2990	486.8387	938.1377	399.5517576	437.9651	0.4380	132.5599	4.621171	21.35522	114.6113	9.35
105	37.6033	449.9703	489.1924	939.1627	397.3535869	434.9569	0.4350	132.5370	4.682829	21.92888	114.5915	9.54
106	37.2734	450.2763	489.0315	939.3078	398.9242887	436.1977	0.4362	132.5100	4.673964	21.84594	114.5681	9.53
107	36.7385	419.8504	516.0926	935.9430	401.0844753	437.8230	0.4378	132.4830	4.445889	19.76593	114.5448	8.65
108	37.6938	442.4837	495.7915	938.2752	389.7023503	427.3961	0.4274	132.4840	4.764841	22.70371	114.5456	9.70
109	37.8925	436.2650	501.1168	937.3818	389.1022961	426.9948	0.4270	132.5035	4.736793	22.43721	114.5625	9.58
110	39.4321	427.2510	508.7816	936.0326	373.8967383	413.3288	0.4133	130.4573	4.633626	21.47049	112.7933	8.87
111	17.6747	432.2319	508.2614	940.4933	663.5629202	681.2376	0.6812	132.7043	3.270753	10.69782	114.7362	7.29
112	23.3891	602.5460	354.9449	957.4909	668.5083781	691.8974	0.6919	132.2236	3.483018	12.13141	114.3205	8.39
113	18.9945	627.3691	333.4256	960.7946	719.8539772	738.8484	0.7388	133.6771	4.017144	16.13745	115.5773	11.92
114	21.3622	598.7395	358.6926	957.4321	686.7550178	708.1172	0.7081	131.9258	3.504804	12.28365	114.063	8.70
115	10.8815	647.0972	321.0404	968.1376	773.482165	784.3636	0.7844	146.3802	3.323891	11.04825	126.5603	8.67
116	11.1291	656.9856	311.0233	968.0089	802.3547101	813.4838	0.8135	140.8395	3.329714	11.087	121.7698	9.02
117	9.8108	636.9919	330.4317	967.4236	774.6387984	784.4496	0.7844	157.8711	3.263759	10.65212	136.4954	8.36
118	13.5718	563.4095	391.1128	954.5224	732.3867955	745.9586	0.7460	144.0010	3.805093	14.47873	124.5032	10.80

Flow period	Oil avg.	Water Avg.	Gas Avg.	mass den g	mass den w	mass oil d	Liq mix	liq den fr	total mix	S.G	Cv	q/Cv	(q/Cv)sq	dP1
81	895.0	1001.9	47.6	20.2751815	516.651677	433.4647	950.1164	545.0383	565.3134	0.5653	124.5482	3.314491	10.98585	6.210448
82	894.7	1001.6	46.9	22.4365934	514.657584	435.0152	949.6727	495.0331	517.4697	0.5175	124.5407	3.668194	13.45565	6.962891
83	893.6	1001.5	49.1	26.4122474	492.115048	454.4928	946.6078	437.211	463.6232	0.4636	123.4094	3.223888	10.39345	4.818647
84	893.7	1001.5	48.9	26.4643863	492.795648	453.9328	946.7284	434.0296	460.494	0.4605	123.4981	3.248817	10.55481	4.860427
85	893.6	1001.8	50.3	25.9851714	499.656422	447.8959	947.5523	458.1967	484.1819	0.4842	123.7327	3.076545	9.46513	4.582845
86	897.4	1004.4	54.0	23.8345746	573.660876	384.8574	958.5183	535.3529	559.1874	0.5592	122.8364	3.107049	9.653751	5.398256
87	896.6	1004.8	57.9	17.8199163	564.544916	392.8244	957.3694	662.9183	680.7383	0.6807	123.5004	2.976707	8.860784	6.031874
88	896.7	1004.8	57.9	17.5956205	569.245258	388.7259	957.9711	666.9873	684.5829	0.6846	123.7682	2.966716	8.801403	6.02529
89	893.8	1001.9	50.5	26.1732335	491.174994	455.6479	946.8229	455.9864	482.1597	0.4822	123.7058	3.280337	10.76061	5.188331
90	895.8	1001.9	45.3	18.5457335	516.840895	433.7041	950.545	560.9696	579.5153	0.5795	124.4912	3.128408	9.786935	5.671679
91	894.0	1002.0	50.6	26.2140255	490.897175	455.996	946.8932	456.2897	482.5038	0.4825	123.6937	3.30573	10.92785	5.27273
92	895.0	1001.9	47.6	20.2751815	516.651677	433.4647	950.1164	545.0383	565.3134	0.5653	124.5228	3.315167	10.99033	6.212981
93	893.8	1001.9	50.6	26.2440208	489.116695	457.4908	946.6075	455.3011	481.5451	0.4815	123.7001	3.293401	10.84649	5.223076
94	894.7	1001.6	46.9	22.4365934	514.657584	435.0152	949.6727	495.0331	517.4697	0.5175	124.5508	3.667897	13.45347	6.961761
95	894.7	1003.0	54.0	17.2906631	444.102828	498.5651	942.6679	641.0008	658.2915	0.6583	124.5149	3.167436	10.03265	6.604408
96	896.9	1004.2	54.6	23.9552108	612.726757	349.6734	962.4001	539.9296	563.8848	0.5639	125.2958	3.42416	11.72487	6.611477
97	898.2	1004.7	53.4	21.9721218	552.882147	403.9187	956.8008	563.3823	585.3544	0.5854	123.9800	3.115369	9.705525	5.681172
98	897.8	1004.5	53.1	22.4483746	552.398804	404.0679	956.4667	551.9142	574.3626	0.5744	125.6251	3.25337	10.58442	6.079292
99	900.1	1005.0	49.9	12.2054672	624.782673	340.5009	965.2836	728.9462	741.1517	0.7412	124.6999	3.179922	10.11191	7.494455
100	897.4	1004.4	54.2	23.7326277	575.686882	383.0264	958.7133	538.7926	562.5253	0.5625	123.9384	3.171522	10.05855	5.658191
101	897.4	1004.4	54.0	23.8345746	573.660876	384.8574	958.5183	535.3529	559.1874	0.5592	122.5299	3.114822	9.702115	5.425301
102	896.6	1004.8	57.9	17.8199163	564.544916	392.8244	957.3694	662.9183	680.7383	0.6807	123.2934	2.981704	8.89056	6.052144
103	894.1	1002.2	51.0	28.8415124	474.458855	470.7902	945.249	410.443	439.2845	0.4393	132.5818	4.631506	21.45085	9.423027
104	895.1	1002.4	49.6	28.4504859	451.769395	491.6848	943.4542	401.8161	430.2666	0.4303	132.5599	4.621171	21.35522	9.188438
105	896.3	1002.9	48.8	28.1406234	450.415094	493.7926	944.2077	399.4881	427.6287	0.4276	132.5370	4.682829	21.92888	9.377421
106	896.4	1002.9	48.6	27.9561809	450.71622	493.5742	944.2904	401.0404	428.9966	0.4290	132.5100	4.673964	21.84594	9.371834
107	896.5	1002.9	48.3	27.6114696	420.259355	520.8352	941.0946	403.2921	430.9036	0.4309	132.4830	4.445889	19.76593	8.517211
108	896.2	1002.8	48.4	28.287656	442.920876	500.3906	943.3115	391.7941	420.0818	0.4201	132.4840	4.764841	22.70371	9.537413
109	896.0	1002.7	48.5	28.3956951	436.698241	505.804	942.5022	391.2278	419.6235	0.4196	132.5035	4.736793	22.43721	9.415179
110	895.8	1002.7	49.0	29.414915	427.698274	513.6976	941.3959	376.0391	405.454	0.4055	130.4573	4.633626	21.47049	8.705296
111	899.1	1003.9	46.3	13.6380482	432.417859	511.8011	944.219	666.1916	679.8296	0.6798	132.7043	3.270753	10.69782	7.272697
112	897.6	1004.4	53.7	16.218469	602.817139	358.8912	961.7083	671.4529	687.6714	0.6877	132.2236	3.483018	12.13141	8.342424
113	897.8	1004.5	53.7	13.4613556	627.607953	336.8312	964.4391	722.5845	736.0459	0.7360	133.6771	4.017144	16.13745	11.8779
114	897.9	1004.5	53.1	15.0180964	598.997621	362.4654	961.463	689.6463	704.6644	0.7047	131.9258	3.504804	12.28365	8.655853
115	904.8	1006.4	44.8	9.00372837	647.430227	322.7062	970.1364	775.0791	784.0828	0.7841	146.3802	3.323891	11.04825	8.662746
116	902.3	1006.0	50.1	8.57082934	657.036464	313.0058	970.0423	804.0401	812.6109	0.8126	140.8395	3.329714	11.087	9.009414
117	904.5	1005.6	41.5	8.27606195	637.021029	331.5638	968.5849	775.5687	783.8447	0.7838	157.8711	3.263759	10.65212	8.349611
118	898.7	1003.2	44.1	10.2594606	563.554373	393.819	957.3734	734.5743	744.8338	0.7448	144.0010	3.805093	14.47873	10.78425